Climate Forcing by Changing Solar Radiation

JUDITH LEAN

E. O. Hulburt Center for Space Research, Naval Research Laboratory, Washington, D.C.

DAVID RIND

Goddard Institute for Space Studies, National Aeronautics and Space Administration, New York, New York

(Manuscript received 7 March 1996, in final form 19 June 1997)

ABSTRACT

By how much does changing radiation from the sun influence the earth's climate, presently and in the recent past, compared with other natural and anthropogenic processes? Current knowledge of the amplitudes and timescales of solar radiative output variability needed to address this question is described from contemporary solar monitoring and historical reconstructions. The 17-yr observational database of space-based solar monitoring exhibits an 11-yr irradiance cycle with amplitude of about 0.1%. Larger amplitude solar total radiative output changes—of 0.24% relative to present levels—are estimated for the seventeenth-century Maunder Minimum by parameterizing the variability mechanisms identified for the 11-yr cycle, using proxies of solar and stellar variability. The 11- and 22-yr periods evident in solar activity proxies appear in many climate and paleoclimate records, and some solar and climate time series correlate strongly over multidecadal and centennial timescales. These statistical relationships suggest a response of the climate system to the changing sun. The correlation of reconstructed solar irradiance and Northern Hemisphere (NH) surface temperature anomalies is 0.86 in the preindustrial period from 1610 to 1800, implying a predominant solar influence. Extending this correlation to the present suggests that solar forcing may have contributed about half of the observed 0.55°C surface warming since 1900 and one-third of the warming since 1970. Climate model simulations using irradiance reconstructions provide a tool with which to identify potential physical mechanism for these implied connections. An equilibrium simulation by the Goddard Institute for Space Studies GCM predicts an NH surface temperature change of 0.51°C for a 0.25% solar irradiance reduction, in general agreement with the preindustrial parameterization. But attributing a significant fraction of recent climate warming to solar forcing presents serious ambiguities about the impact of increasing greenhouse gas concentrations whose radiative forcing has been significantly larger than solar forcing over this time period. Present inability to adequately specify climate forcing by changing solar radiation has implications for policy making regarding anthropogenic global change, which must be detected against natural climate variability.

1. Introduction

Earth's climate fluctuates (Bradley 1991; Hartmann 1994). Volcanic eruptions and the sun's activity are potential causes of natural climate change (Hansen and Lacis 1990), as are internal oscillations and couplings between the ocean and the atmosphere (Rind and Overpeck 1993; Crowley and Kim 1993; Mehta and Delworth 1995). Industrial activity and associated trace gas releases may also be altering the earth's climate (Houghton et al. 1992; Houghton et al. 1995). Necessary for reliable detection of suspected anthropogenic climate change is proper specification of natural climate fluctuations that are occurring independently of human activities.

Corresponding author address: Dr. Judith Lean, Naval Research Laboratory, Code 7673L, Washington, DC 20375.
E-mail: lean@demeter.nrl.navy.mil

Concern abounds that the 0.55°C increase in the global surface temperature of the earth during the past century (Parker et al. 1994) may signify the climate system's response to anthropogenic influences that have escalated during the industrial epoch (Kuo et al. 1990; Hansen et al. 1993; Visser and Molenaar 1995). Instrumental records, shown in Fig. 1, document this temperature increase globally (land plus ocean) and in both the Northern and Southern Hemispheres (NH and SH; Houghton et al. 1992). The temporal structure of the observed warming is clearly more complicated than the simple upward trend expected from monotonically increasing annual greenhouse gas concentrations alone (e.g., Lau and Weng 1995). The warming is also geographically complex (Parker et al. 1994)—significant variance exists at multiannual and decadal timescales with different amplitudes at different locations, sometimes masking the upward trend (Allen and Smith 1994; Mann and Park 1994).

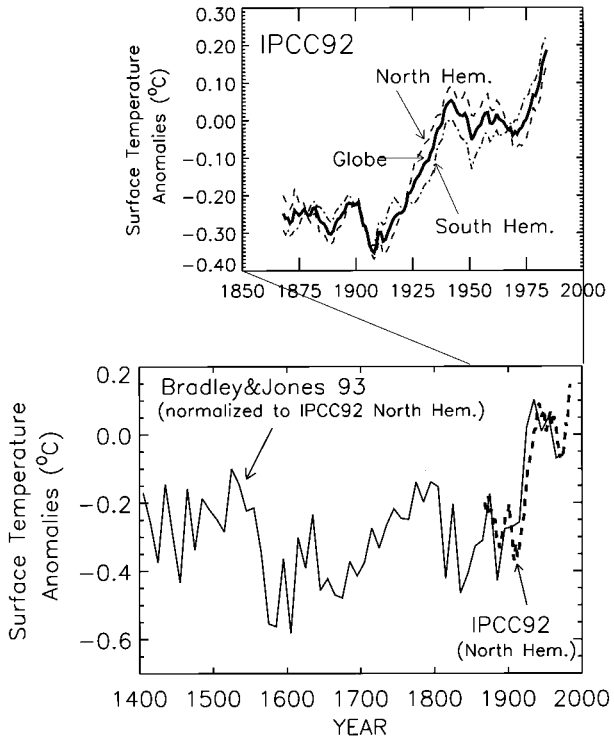

FIG. 1. The IPCC (Houghton et al. 1992) instrumental record of surface temperature anomalies since 1870 is shown in the upper panel for the globe (solid line) and the Northern (dashed line) and Southern (dashed–dotted line) Hemispheres. In the lower panel, the solid line is a reconstruction of NH summer surface temperature anomalies since 1400 (Bradley and Jones 1993), scaled to match decadally averaged IPCC (Houghton et al. 1992) NH (dashed line) in the overlap period. The scaling used is BJ93 = 0.55 + 3.56 × IPCC92.

It is a challenging task to identify the natural and anthropogenic causes of twentieth century climate change with the scientific certainty needed for environmental policy making. A recent paleoreconstruction of NH summer surface temperatures (Bradley and Jones 1993), also shown in Fig. 1, suggests that the twentieth century warming may actually be part of a longer-term, larger amplitude warming that commenced in the seventeenth century, prior to the industrial epoch. During a period from roughly 1450 to 1850—loosely called the Little Ice Age—surface temperatures were at times cooler by as much as 0.7°C than present, especially in northern Europe (Bradley and Jones 1993; Damon and Jirikowic 1994) (e.g., near 1600 in Fig. 1). Rather than a response to anthropogenic influences, the warming since the Little Ice Age might signify the climate's recovery to warmer temperatures as may have been present in the twelfth century so-called Medieval Climatic Maximum (Hughes and Diaz 1994) that preceded it.

Since 1850, industrially produced concentrations of greenhouse gases—CO_2, CH_4, N_2O, chloroflurocarbons (CFCs)—and of tropospheric sulfate aerosols, have increased (Houghton et al. 1995). The overall activity level of the sun has risen, too (NRC 1994). Earth's surface is warmed both by increased greenhouse gas concentrations and the enhanced solar radiation speculated to accompany the sun's increased activity, since both input additional energy in the climate system. In contrast, increasing atmospheric aerosol concentrations are expected to cool the earth's surface by reflecting more of the sun's radiant energy back to space. Whereas surface cooling is expected from tropospheric industrial aerosols, which have increased in the past century (Penner et al. 1994; Penner et al. 1995), the amount of aerosols injected into the stratosphere by volcanoes decreased for much of the twentieth century (Lamb 1977; Sato et al. 1993; Robock and Free 1995), contributing to surface warming by allowing sunlight to warm the earth's surface, unobstructed by atmospheric aerosol scattering, reflection, or absorption.

Changing atmospheric ozone concentrations further complicates the interpretation of recent climate change. Surface cooling is expected in the past few decades from the depletion of stratospheric ozone by CFCs since ozone is a greenhouse gas (Schwarzkopf and Ramaswamy 1993) as well as Earth's biological ultraviolet shield (de Gruijl 1995). At the same time, anthropogenic tropospheric ozone increases contribute to surface warming (Lacis et al. 1990). Since changing solar UV radiation modulates ozone concentrations (Hood and McCormack 1992; Hood et al. 1993; Chandra and McPeters 1994; Haigh 1994; Hood 1997), the ozone influence on climate exhibits both natural and anthropogenic components. Surface albedo is changing too, in response to altered land use patterns (Hannah et al. 1994).

Climate responds differently to individual forcings—greenhouse gases, aerosols, ozone, solar variability—because the forcings have distinct regional and altitude distributions, different temporal histories, illustrated in Fig. 2, and different magnitudes, summarized in Fig. 3. Of the various natural and anthropogenic climate forcings, only that by greenhouse gases (particularly CO_2) is reasonably well specified over the past 150 yr. Sometimes construed from this lack of knowledge of other influences is the assumption that none but greenhouse gases are significant for recent climate change. However, assuming climate sensitivity κ is in the accepted range 0.3–1.0°C per W m^{-2}, an interpretation of surface warming over the past century based solely on greenhouse gas forcing is inconsistent with observations. A temperature increase $\Delta T = \kappa \Delta F$ in the range 0.7°C–2.4°C is expected from a greenhouse gas forcing of $\Delta F = 2.4$ W m^{-2} over the past 150 yr, in excess of the actual observed 0.55°C warming. Clearly, present knowledge of climate sensitivity is inadequate for translating greenhouse gas radiative forcing to surface warming. This implies that other forcings, though poorly specified, may be important for interpreting recent climate change. Even the speculated net climate forcing of 1.2 W m^{-2} shown in Fig. 3 for the past 150 yr predicts an average

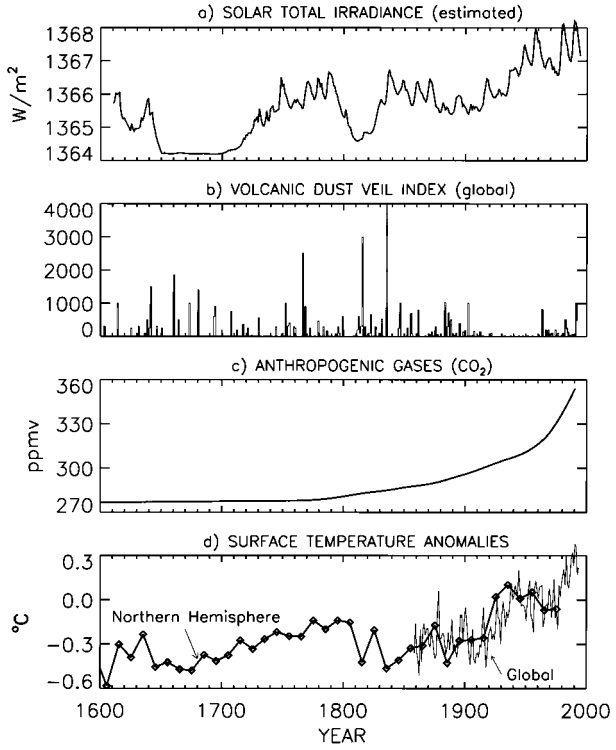

FIG. 2. Both natural and anthropogenic influences are suspected of modifying the earth's climate during the past four centuries. Compared are annual averages of (a) estimated solar total irradiance (Lean et al. 1995b), (b) the volcanic aerosol loading according to the global dust veil index (Lamb 1977; Robock and Free 1995), and (c) the concentration of CO_2 (Keeling and Whorf 1994). The Bradley and Jones (1993) record of decadal NH surface temperature, shown in (d), suggests that the warming recorded by the IPCC (Houghton et al. 1992) data from Fig. 1 over the past 150 yr is part of a longer term trend that commenced prior to the industrial revolution. Nor has the warming, which exhibits significant variance in addition to an overall upward long-term trend, tracked in detail the monotonically increasing annual greenhouse gas concentrations.

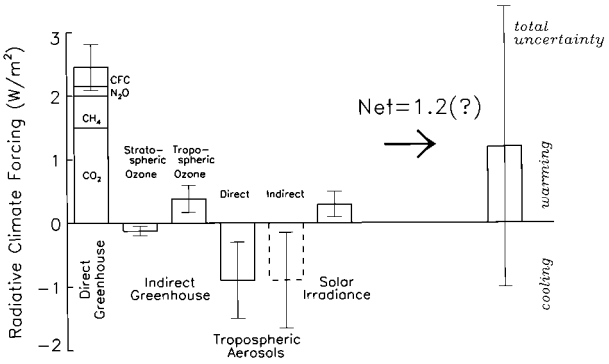

FIG. 3. Amplitudes of the natural and anthropogenic climate forcings estimated for the past 140 yr, from 1850 to 1990, are shown from IPCC (Houghton et al. 1995). Each individual forcing is expected to impact the climate system in different ways depending on its latitude, altitude, and history. However, climate change assessments lack the complexity to account for the myriad pathways of the climate system response, and global-scale studies often assume a common climate sensitivity to the different forcings (see also, Hansen et al. 1983). With this assumption, the data in this figure suggest a net radiative climate forcing of 1.2 W m^{-2} from 1850 to 1990, adopting an indirect aerosol forcing of -1 W m^{-2} (the midpoint of the Houghton et al. 1995 uncertainty range and consistent with the results of Penner et al. 1995).

surface warming somewhat higher than the actual observations, except for low climate sensitivity.

Similarities of surface temperature and solar variability records over decadal timescales, evident in Fig. 2, point to solar forcing as a contributor of recent climate change. Surface temperatures since 1850 are shown in Fig. 4 to correlate well with solar activity (Reid 1991; Friis-Christensen and Lassen 1991; Hoyt and Schatten 1993), with correlation coefficients as high (0.7) as the correlation between surface temperatures and greenhouse gas concentrations (Kelly and Wigley 1992). However, accounting for the entire surface warming by direct solar radiative forcing alone is unlikely: greenhouse gases have increased over this time period, and simulations of a solar warming scenario with simple climate–ocean energy balance models require solar irradiance variations larger than the 0.1% 11-yr irradiance cycle evident in the contemporary solar monitoring database or climate sensitivities in excess of present estimates (Schlesinger and Ramankutty 1992; Kelly and Wigley 1992).

Understanding solar influences on climate requires improved specification of both the amplitudes and timescales of solar radiative output changes on climatological timescales and the climate sensitivity to small insolation changes. Space-based solar monitoring has documented unequivocally the existence of an 11-yr cycle in the primary energy provided from the sun to the earth (its total radiative output). The possibility of larger amplitude changes over longer timescales that might physically account for significant climate change cannot be dismissed. Knowledge of climate response to the sun's changing solar radiation is rudimentary, encompassed in simple processes that fail to explain climate change observed on timescales from the past century to the 100 000-yr Milankovitch forcing (Rind et al. 1989; Phillips and Held 1994). Present inability to quantify climate forcing by changing solar radiation, whether negligible or significant, is a source of uncertainty that impacts policy making regarding global climate change (George C. Marshall Institute 1989; Houghton et al. 1995).

2. Solar radiative output variability

The sun, whose surface temperature is near 6000 K, provides electromagnetic, particle, and plasma energy to the earth at levels summarized in Table 1. Electromagnetic radiation is by far the largest solar energy source for the earth and the most important for its climate. When the solar spectrum shown in Fig. 5a is integrated over all wavelengths, the total radiative out-

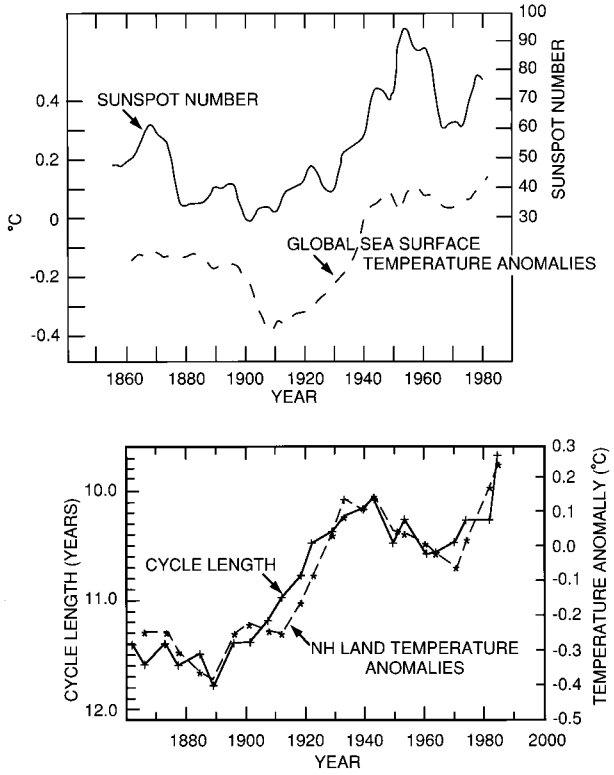

FIG. 4. Correlations are shown between climate data and solar variability proxies. Compared in the upper figure is the 11-yr running mean of the sunspot number with global average sea surface temperature anomalies, from Reid (1991). In a one-dimensional model of the thermal structure of the ocean, consisting of a 100-m mixed layer coupled to a deep ocean, and including a thermohaline circulation, a change of 0.6% in the total solar irradiance S is needed to reproduce the observed variation of 0.4°C in the sea surface temperature anomalies. Compared in the lower figure are the length of the solar cycle (plus signs) with NH land temperature anomalies (asterisks), calculated as averages over individual ''half'' solar cycles (i.e., solar maximum to solar minimum), from Friis-Christensen and Lassen (1991). Note the phase differences of as much as 20 yr between solar cycle length and sunspot number and between sea surface and NH land-surface temperature anomalies.

put from the sun at the earth is 1366 W m^{-2} (with a measurement uncertainty of ± 3 W m^{-2}).

There is no doubt that the sun is an active star. Sunspots exhibit a prominent 11-yr cycle, first reported by Schwabe in 1843, and also shorter (e.g., 27-day rotational) and longer (e.g., 88-yr Gleisburg) cycles. Widely adopted as a proxy of solar activity in many geophysical investigations, the sunspot number is in fact but one record, albeit the longest, of myriad other variable solar magnetic phenomena and their modulation of radiation, particle, and plasma energy outputs. Both the total radiative output and the spectral shape of the radiation change during the sun's activity cycle, as shown by the 11-yr variability amplitudes in Fig. 5b, with the shortest wavelengths varying by many orders of magnitude more than the visible radiation.

Radiation at near-UV, visible, and near-IR wavelengths comprises the bulk of the total radiative output; the sun emits 48% of its radiation at wavelengths between 400 and 800 nm. This radiation is directly available to the earth's surface and troposphere (see Fig. 5a spectrum at 0 km). Shorter wavelength UV radiation and solar energetic particles deposit their energy in the earth's atmosphere, mainly above the troposphere. Atmospheric gases—O_2, N_2, O, and O_3—are strong absorbers of UV radiation. Solar radiative energy at wavelengths increasingly shorter than 300 nm varies with increasingly larger amplitudes and is deposited increasingly higher above the earth's surfaces, at altitudes of unit optical depth (the altitude at which vertically incident sunlight is attenuated to 1/e of its flux on top of the earth's atmosphere) shown in Fig. 5c.

a. Contemporary observations

During the past 17 yr, solar monitors on earth-orbiting spacecraft have detected the sun's changing levels of total (spectrally integrated) and UV spectral radiation throughout the 11-yr activity cycle (Rottman 1988; Willson and Hudson 1991; Hoyt et al. 1992; London et al. 1993; Lee et al. 1995; Chandra et al. 1995; Woods et al. 1996; Lean et al. 1997). The data in Fig. 6 provide irrefutable evidence of the 11-yr total irradiance cycle—the solar ''constant'' is not, in fact, constant. When solar activity is high, as indicated by the sunspot number, so too are the total and UV radiative outputs from the sun (see, e.g., reviews by Lean 1991, 1997). Additional radiative output variations have been detected on timescales of minutes, days, months, and years, superimposed on the overall 11-yr cycle (Hudson 1988; Fröhlich

TABLE 1. Examples of the magnitude and variability of solar sources of terrestrial energy (based on NRC 1994).

Source	Energy (W m^{-2})	Solar cycle change (W m^{-2})	Terrestrial deposition altitude
Solar radiation			
Total irradiance	1366	1.3	surface, troposphere
UV 200–300 nm	15.4	0.16	0–50 km
UV 0–200 nm	0.1	0.02	50–500 km
Particles			
Solar protons	0.002		30–90 km
Galactic cosmic rays	0.000007		0–90 km
Solar wind	0.0003		above 500 km

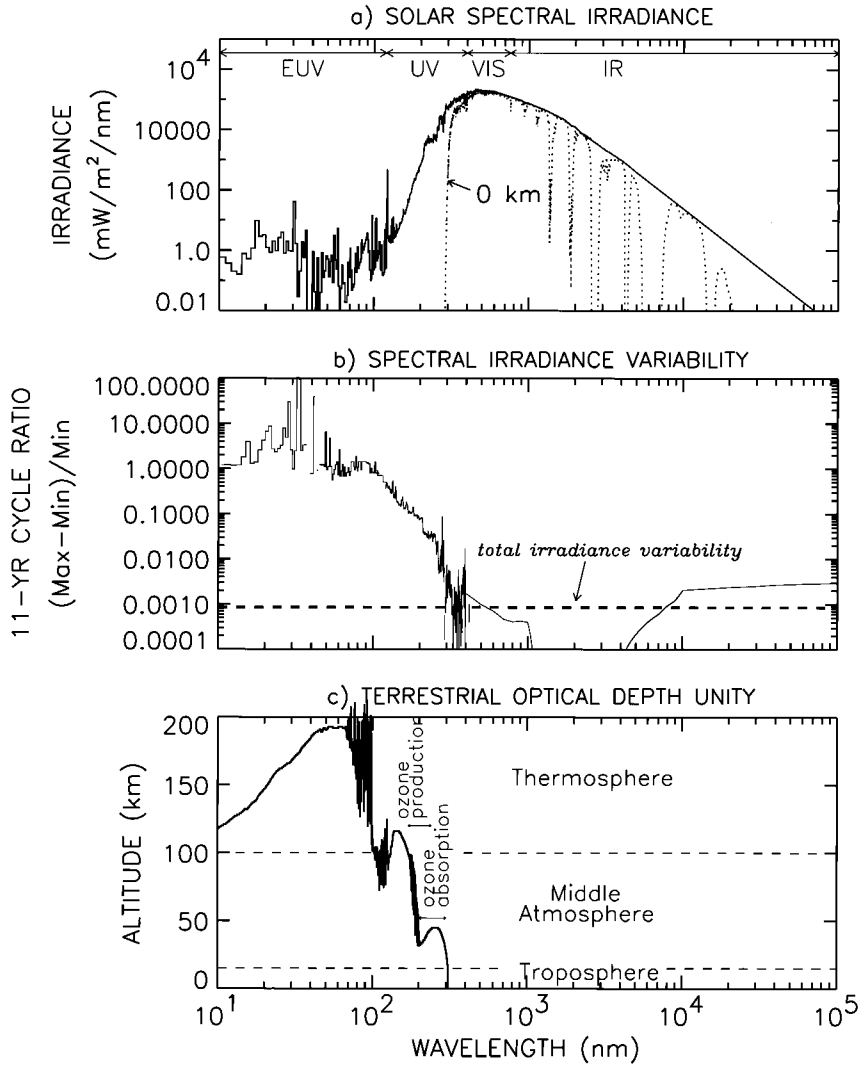

FIG. 5. Shown in (a) is the spectrum of the sun's radiation incident on top of the earth's atmosphere (solid line, typical of solar minimum conditions), and at the earth's surface (0 km, dotted line). The solar total irradiance S is the integral over all wavelengths of the spectrum at the top of the atmosphere. The broad spectral bands identified along the top of this figure are the extreme ultraviolet (EUV), ultraviolet (UV), visible (VIS), and infrared (IR). Not shown, at wavelengths longward of the IR, is the microwave or radio portion of the solar spectrum. Shown in (b) are variations of the solar spectrum estimated for a recent 11-yr activity cycle. At wavelengths longer than 400 nm, these estimates are speculative because no observational data exist. The dashed line indicates the solar cycle variation in the spectrally integrated (i.e., total) solar irradiance. Deposition of the sun's radiative energy in the earth's atmosphere depends on the wavelength of the radiation, as shown in (c) where the altitude at which the incident energy from an overhead sun is attenuated by a factor of 1/e (unit optical depth) is plotted as a function of wavelength. Also indicated are the wavelength regions which dominate ozone production and absorption. Adapted from Lean (1991), updated with the recent near-UV variability estimates of Lean et al. (1997).

et al. 1991; Fröhlich et al. 1997). Evident in Fig. 6, for example, are excursions of a few tenths percent associated with the sun's 27-day rotation, superimposed on the more slowly varying 0.1% 11-yr irradiance cycle. The present database is yet too short to resolve the amplitudes of longer period irradiance changes that may be occurring as well (Lee et al. 1995).

Knowledge of the 11-yr irradiance cycle is presently imperfect. Compounded with uncertainties arising from the limited duration of space-based solar monitoring, which barely exceeds one 11-yr cycle, are instrumental uncertainties that cause spurious variability signals in individual solar radiometers. Radiometer sensitivity changes are often pronounced during the first year of

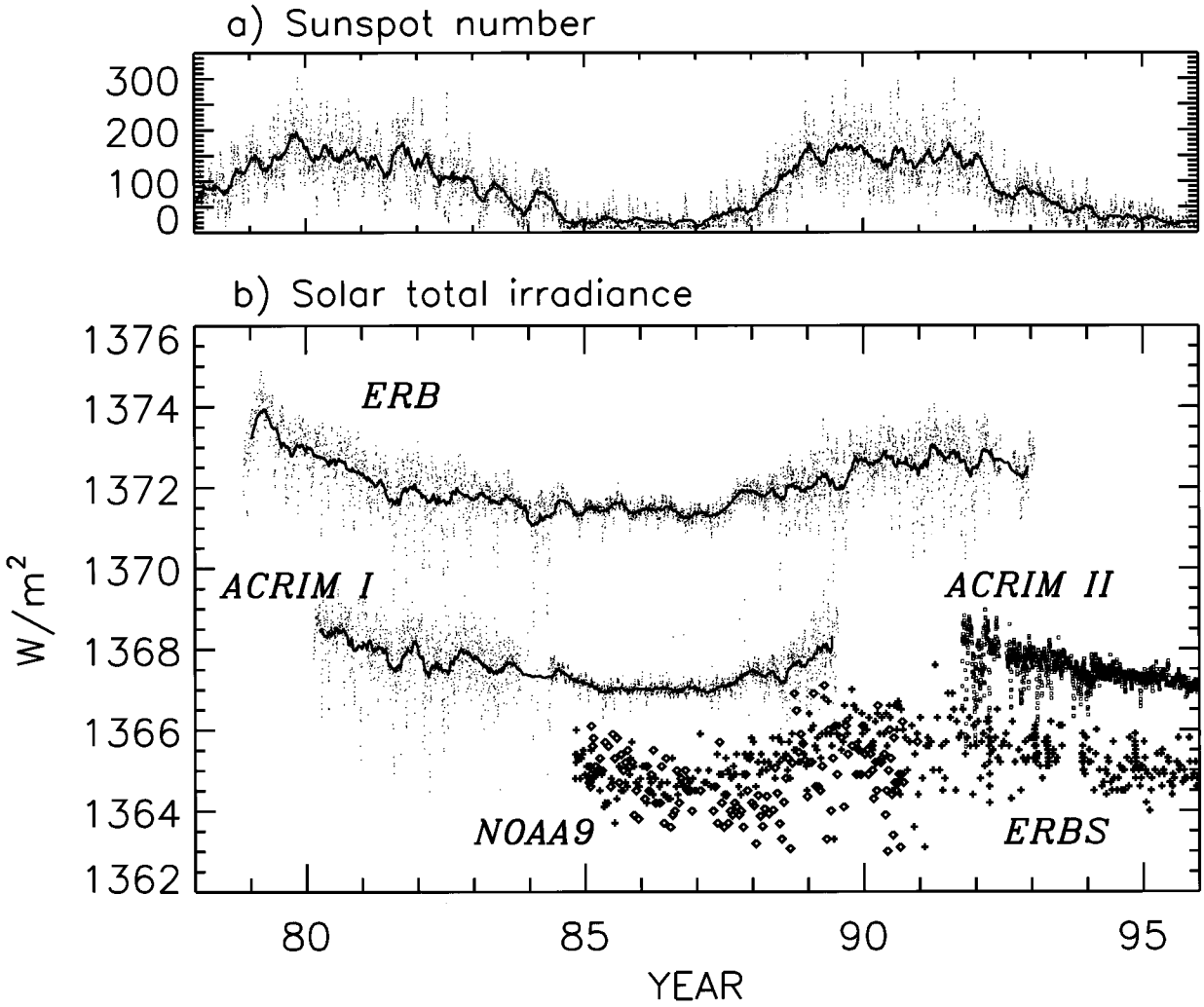

FIG. 6. Contemporary solar activity variations are indicated by the sunspot number in (a) and changes in total solar radiative output in (b), recorded by the ERB radiometer on the *Nimbus-7* satellite, ACRIM I on the *Solar Maximum Mission* (*SMM*) satellite, and ACRIM II on the *UARS*, and by the ERBE program (*NOAA-9* and *ERBS*). The solid lines in (a) and (b) are 81-day running means of the daily data, which are shown as dots. The absolute irradiance scale of the ACRIM II data has been adjusted to match that of ACRIM I using the overlapping ERBS data. Solar total irradiance increases during times of maximum solar activity (e.g., 1980 and 1990) relative to its levels in the intervening activity minimum. The differences in absolute irradiance levels among the different measurements are of instrumental origin and reflect absolute inaccuracies in the measurements. Because these inaccuracies exceed the solar cycle amplitude, the cross-calibration of successive radiometers is mandatory to preserve the historical irradiance database.

space deployment because the solar flux incident on the instrument modifies surface contaminants, altering the spectral absorptivity and reflectivity of the instrument's optical components (Luther et al. 1986). This may explain the pronounced decrease in 1979 of the Earth Radiation Budget (ERB) measurements made from the *Nimbus-7* spacecraft (Hoyt et al. 1992). Likewise, instrumental changes may have caused the distinct upward trend in 1992 at the beginning of the Active Cavity Radiometer Irradiance Monitor (ACRIM) measurements on board the *Upper Atmosphere Research Satellite* (*UARS*), which are not replicated by either the simultaneous ERB or *Earth Radiation Budget Satellite* (*ERBS*) data, both of which had been operating for much longer. Instrumental factors possibly caused by sensitivity changes related to temperature or aspect drifts are also implicated in the discrepancies between ERB and *ERBS* data during 1990–92, near the peak of solar cycle 22 (Lee et al. 1995). But despite these individual instrumental discrepancies, the basic features of the 11-yr irradiance cycle and higher frequency variability emerge clearly, by virtue of the multiple, overlapping, cross-calibrated measurements that comprise the extant database.

The sun's irradiance fluctuates because, as illustrated in the solar images in Fig. 7, radiation sources are not homogeneously distributed on its disk. Magnetic fields erupting from the solar convection zone into the over-

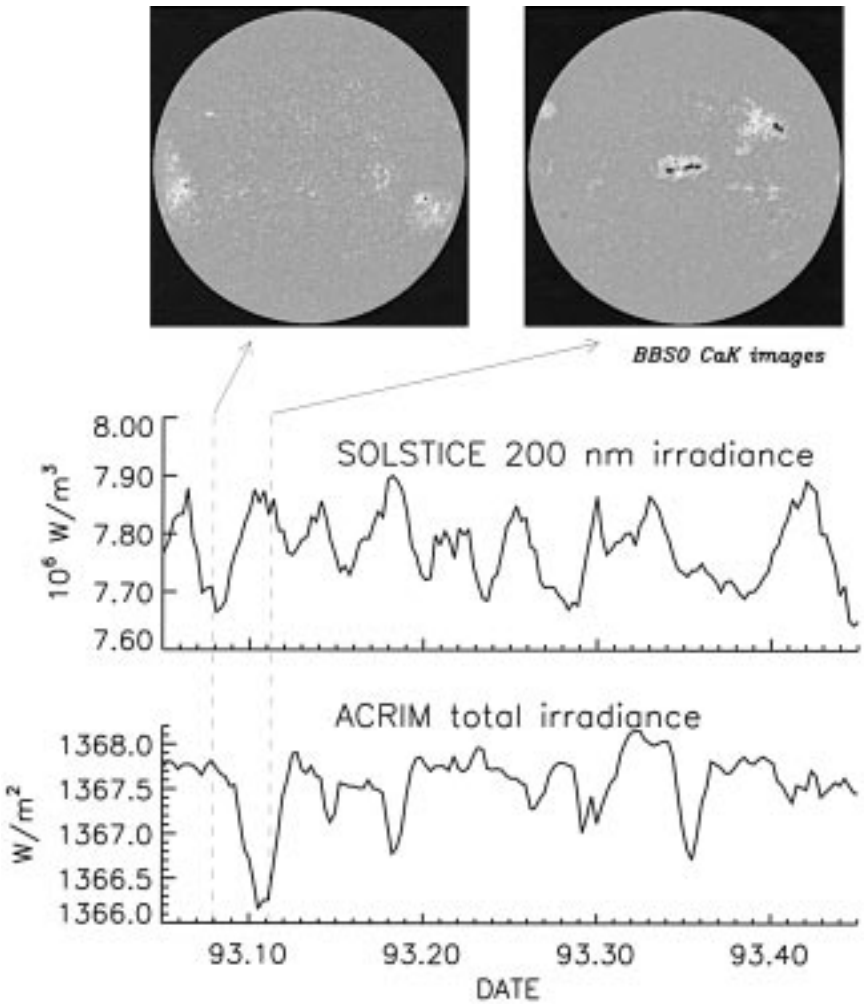

FIG. 7. Magnetic active regions are evident in images of the sun recorded at the Big Bear Solar Observatory in the emission of singly ionized calcium (Ca II). Dark sunspots and bright plages occur where the local radiation is respectively darker and brighter than from the surrounding solar disk. As the sun rotates on its axis (with a period of about 27 days), the magnetic active regions appear to move across the face of the sun's disk seen at the earth. In the image on the left, on 29 Jan 1993, there are fewer active regions than in the image on the right, on 10 Feb 1993. Changing surface magnetic activity modulates the radiation emitted from the sun, and is evident in the total (lower panel) and UV (upper panel) irradiance time series recorded, respectively, by the ACRIM and Solar Stellar Irradiance Comparison Experiment instruments on *UARS*. Over the short timescales of solar rotation, sunspot effects dominate the total radiative output whereas the UV irradiance variations respond mainly to plage effects—causing the total irradiance to decrease and UV irradiance to increase between 29 Jan and 10 Feb 1993.

lying solar atmosphere generate active regions and complexes in which the local radiation is altered relative to the background solar disk. Both dark sunspots and bright plages are evident in Fig. 7. Magnetic activity erupts, evolves and decays at different rates throughout the 11-yr cycle, generating sunspots, plages, and faculae and a bright emission network that continuously modulate solar total and spectral radiative output (see, e.g., Foukal 1990; Lean 1991), demonstrated in Fig. 7 by the irradiance time series.

Dark sunspots on the solar disk reduce total radiative output (e.g., on 10 February 1993, the right-hand image in Fig. 7) because their emission is less than that of the surrounding disk (Hudson et al. 1982). As the sun rotates, the sunspots appear to move across and off the face of the disk projected toward the earth, modulating solar total irradiance by as much as a few tenths percent on timescales of days to weeks. Although sunspots are the prime cause of 27-day rotational modulation, they are not the only source of irradiance variability; if they were, then the sun would be dimmer instead of brighter during times of high activity when sunspots occur much more frequently, which is not the case (see Fig. 6).

Magnetic regions where emission is enhanced (rather

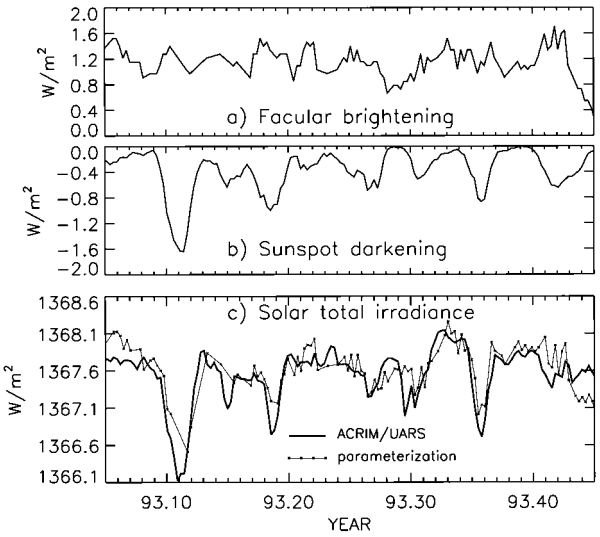

FIG. 8. Shown are parameterizations during 1993 (for the time period of Fig. 7) of (a) the bolometric facular brightening and (b) the sunspot darkening responsible for the predominant variations in total solar irradiance. The sunspot darkening is calculated from information about sunspot areas and positions obtained from ground-based visible light solar images. The facular brightening is parameterized from a ground-based facular proxy (the He 1083-nm equivalent width data) using a correlation with the ACRIM I data from which the sunspot blocking has been removed (after Foukal and Lean 1988). The agreement in (c) between the net parameterization and the total solar irradiance observed by ACRIM confirms that the combined sunspot darkening and facular brightening replicate much of the observed total irradiance variations on solar rotational timescales.

than depleted, as in sunspots), called plages and faculae also contribute to rotational modulation, as shown in Fig. 8, because they too are inhomogeneously distributed on the face of the sun. These regions are evident as complexes of bright emission called plages in the Ca solar images in Fig. 7. When viewed in visible emission they are identified as faculae, the photospheric footprints of the chromospheric plages. As well, small-scale elements form a network of bright emission over the solar disk that changes throughout the solar cycle but is relatively well dispersed in heliographic latitude, contributing minimally to rotational modulation but significantly to solar cycle variability. Bright facular and network emission variations more than compensate for sunspot darkening over the longer timescales of the 11-yr cycle (Foukal and Lean 1988; Lean et al. 1998), as shown in Fig. 9. Although faculae have less magnetic flux than in spots, they extend over considerably more of the sun's disk and persist longer. Changes in global solar structure separate from the magnetic sunspots, faculae, and network are speculated to also affect radiative output (Kuhn and Libbrecht 1991; but see also Solanki and Unruh 1998 for counterarguments). While the actual detailed identification of the bolometric (spectrally integrated) brightness sources of solar radiative output variability is not yet complete, it is now well established that the net result is a solar cycle total irradiance modulation approximately twice that of sunspots.

The shape of the entire solar radiation spectrum also varies with solar activity. The competing effects of dark sunspots and bright faculae, whose bolometric variations are shown in Fig. 9, change as a function of wavelength, with the result that the amplitude of the spectrum variability is wavelength dependent (Fig. 5b). Total radiative output typifies the behavior of radiation at visible wavelengths (where solar spectral flux peaks; see Fig. 5a) for which the 11-yr variation in bright facular emission is about twice the sunspot emission depletion (Fig. 9). Progressing to shorter UV wavelengths, the facular brightening becomes increasingly larger relative to sunspot darkening (Lean 1989; Lean et al. 1997). For example, facular brightness variations control almost entirely the radiation variability at 200 nm (Fig. 7) over both the 27-day and 11-yr cycles, with little detectable sunspot modulation.

b. Historical reconstructions

Lack of direct solar monitoring for all but the last 17 yr, an extremely short epoch climatologically, motivates the reconstruction of historical irradiance variations from proxy records of solar activity that are available over much longer epochs. The reconstructions rely on proper identification of irradiance variability sources in the contemporary solar monitoring database and parameterization of the variability of these sources using the proxy records.

Clearly, the net solar total irradiance shown in Fig. 6b varies approximately in phase with solar activity, shown in Fig. 6a, but the connection of irradiance and sunspot number is not direct. Figure 9 shows that the amplitude of the irradiance variability in each 11-yr cycle depends on the relative strengths of the sunspot and facular irradiance modulation, which can each have different relationships to the sunspot number in different activity cycles. A reconstruction since 1874 of solar total irradiance modulation by the 11-yr cycle in which sunspot darkening and facular brightening are parameterized separately is shown in Fig. 10. Sunspot darkening is calculated directly from white light observations of sunspot areas and locations made primarily by the Greenwhich Observatory (following Foukal 1981). Facular brightening is parameterized from observations by ACRIM on the *Solar Maximum Mission* (*SMM*) spacecraft by correlating monthly mean values of the measured irradiance corrected for sunspot darkening (called the residual irradiance) with monthly mean sunspot numbers (following Foukal and Lean 1990). Physically, this correlation reflects the occurrence of large facular complexes in the vicinity of magnetic active regions that also contain groups of sunspots.

In contrast to the sunspot number record of historical solar activity, which has a pronounced 11-yr cycle but no perceptible overall long term trend, shown in Fig.

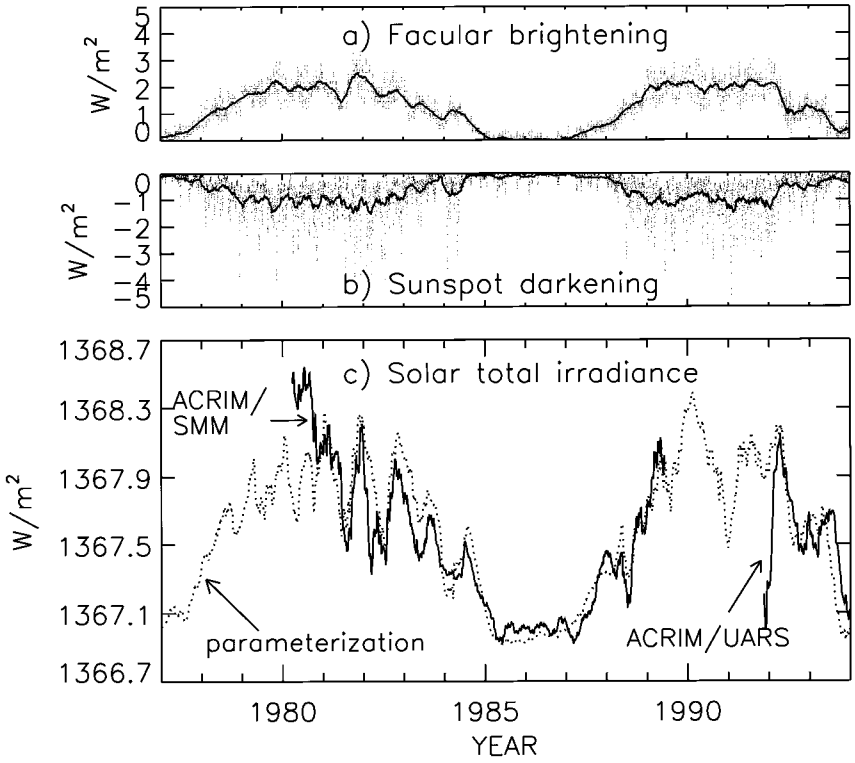

FIG. 9. Shown are the contributions to total solar radiative output variability of (a) the bolometric facular brightening and (b) the sunspot darkening. Daily data are shown as dots and the solid lines are 81-day running means. The general agreement in (c) between the net parameterization (dotted line) of these two competing mechanisms and the total solar irradiance observed by the ACRIM instruments (solid line) confirms that sunspots and faculae cause the predominant variations in total solar irradiance during the 11-yr solar activity cycle (from Lean et al. 1995b). In this figure, the ACRIM data from the *SMM* and *UARS* spacecraft are cross-calibrated using overlapping *ERBS* measurements, as shown in Fig. 6.

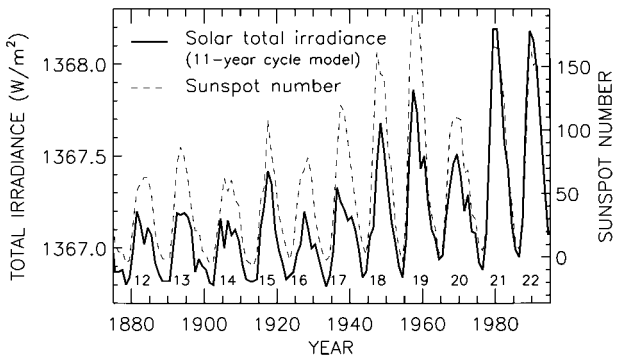

FIG. 10. Compared with the annual mean sunspot number (dashed line) are variations in annual mean solar total irradiance associated with the 11-yr cycle (only) (solid line), calculated with an empirical model developed by Foukal and Lean (1990), which utilizes separate parameterizations for sunspot darkening and facular brightening effects. Note that although the sunspot number was higher in cycle 19 than for subsequent cycles 20–22, solar total irradiance was not, according to the irradiance model. However, this may not be a true solar effect but rather an artifact in the sunspot blocking record (which underwent instrumental changes in 1976) (Fligge and Solanki 1997).

11 (top panel) is a high resolution time series of solar activity recorded by ^{10}Be cosmogenic isotopes in a Greenland ice core (Beer et al. 1988; Beer et al. 1994). An 11-yr cycle superimposed on a longer-term variability component is evident in ^{10}Be, and also in the geomagnetic solar activity indices since 1874 (Joselyn 1995). Ice core ^{10}Be and tree ring ^{14}C (Stuiver and Braziunas 1993) are formed by galactic cosmic ray ionization of gases in the earth's atmosphere that are subsequently incorporated in tropospheric processes. Solar activity modulates cosmogenic isotope production because magnetic coupling between the sun and the earth facilitated by the solar wind plasma is more complex when solar activity is high, inhibiting the flow of galactic cosmic rays to the terrestrial environment and reducing the concentrations of cosmogenic isotopes relative to times of low solar activity. Since solar activity modulates the sun's radiative output, as evidenced during the 11-yr cycle, irradiance changes might also accompany the longer-term solar activity changes recorded by the cosmogenic isotopes (Fig. 11, bottom panel).

In addition to an 11-yr activity cycle, cosmogenic isotope archives exhibit periods near 88 (the Gleisburg

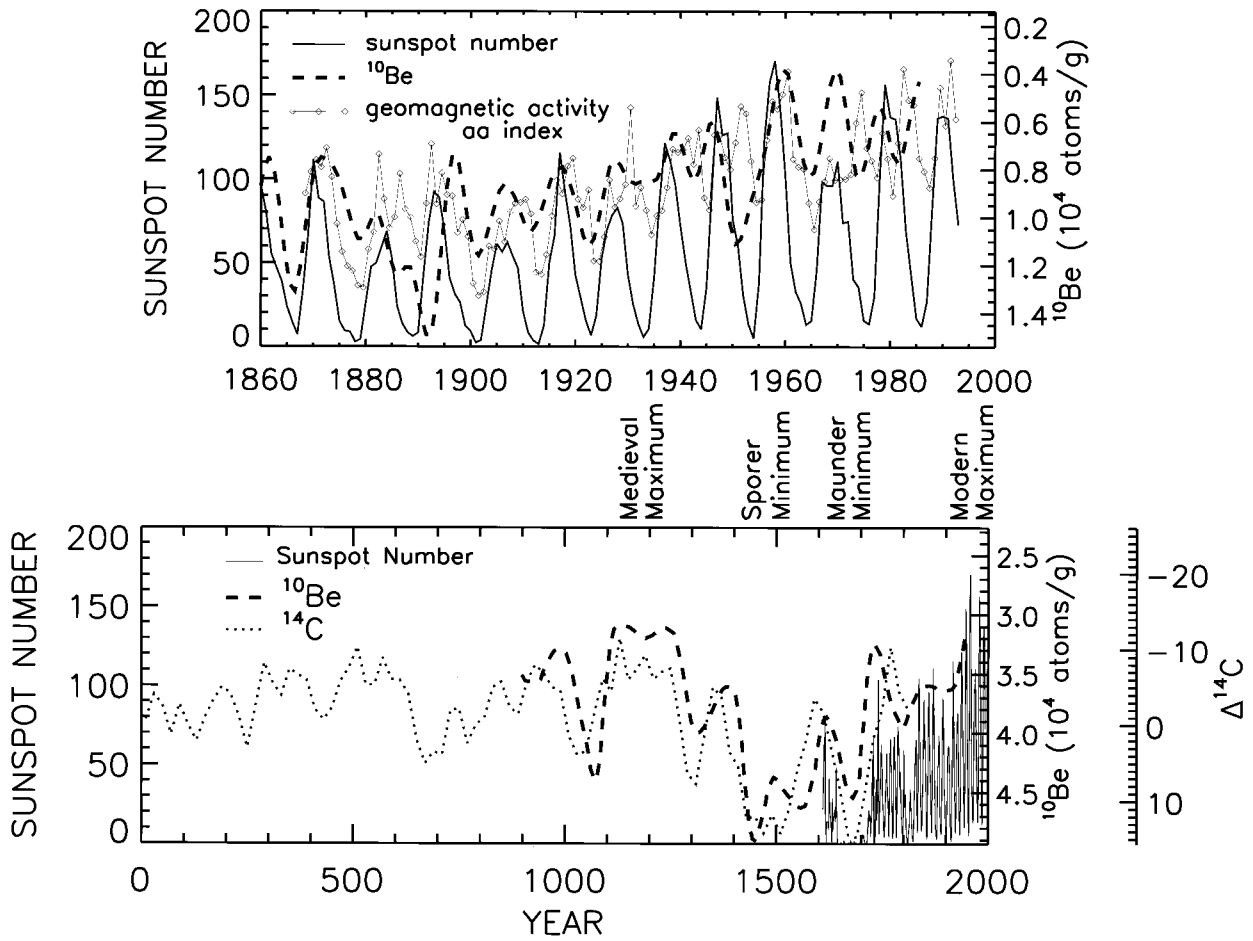

FIG. 11. Compared in the upper figure are three different records of solar variability during the past 130 yr. Unlike the sunspot number (solid line) whose values at cycle minima remain essentially flat (near zero), both the aa geomagnetic index (diamonds) and the ^{10}Be cosmogenic isotopes (thick dashed line) exhibit 11-yr cycles superimposed on steadily increasing longer-term trends. Shown in the lower figure are centennial timescale variations in solar activity over the past 2000 yr seen in both the ^{10}Be (dashed line) and ^{14}C (dotted line) cosmogenic isotopes, which track the envelope of the sunspot numbers (thin solid line) during more recent times (Eddy 1976).

cycle), 210, and 2300 yr (Stuiver and Braziunas 1993; Beer et al. 1994). Furthermore, both tree ring ^{14}C and ice core ^{10}Be data in Fig. 11 document a steady increase in solar activity since the seventeenth century Maunder Minimum (McHague and Damon 1991), perhaps reflecting the net response to solar activity modulation at these longer period cycles. A secular decrease in solar radius of the order of 0.1 arcsec, century^{-1} over the past few centuries (Gilliland 1981; Sofia and Fox 1994; Fiala et al. 1994) may be related to the overall changing solar activity. What amplitude irradiance change might have occurred as well?

Long-term monitoring of ionized Ca emission, a surrogate for magnetic activity in the sun and stars, provides additional evidence that the sun's radiative output may compose a longer-term variability component in addition to the 11-yr cycle. Bright Ca emission seen in the solar images in Fig. 7 is also detected in sunlike stars, and fluctuations in Ca emission occur in some sunlike stars on decadal timescales analogous to the 11-yr solar cycle (Wilson 1978). Some stars, however, have no apparent cycle during the few decades over which they have been monitored. In these stars, the Ca emission is reduced below that of the cycling stars, suggesting perhaps conditions analogous to the sun's Maunder Minimum of anomalously low activity (Baliunas and Jastrow 1990).

Quantitative comparison of solar and stellar brightness changes seen in ionized Ca emission provides a tool for estimating amplitudes of longer term solar radiative output variations. Compared with 13 sunlike stars, the range of Ca emission from the sun during its contemporary 11-yr cycle places it in the brightest one-third of the distribution in Fig. 12 (White et al. 1992). The Ca emission variations on the sun closely track the facular brightness variations that control long-term solar radiative output. When the ACRIM total irradiance observations are corrected for sunspot darkening, the residual irradiances correlate strongly with simultaneously measured Ca fluxes (Livingston et al. 1988), and Ca and

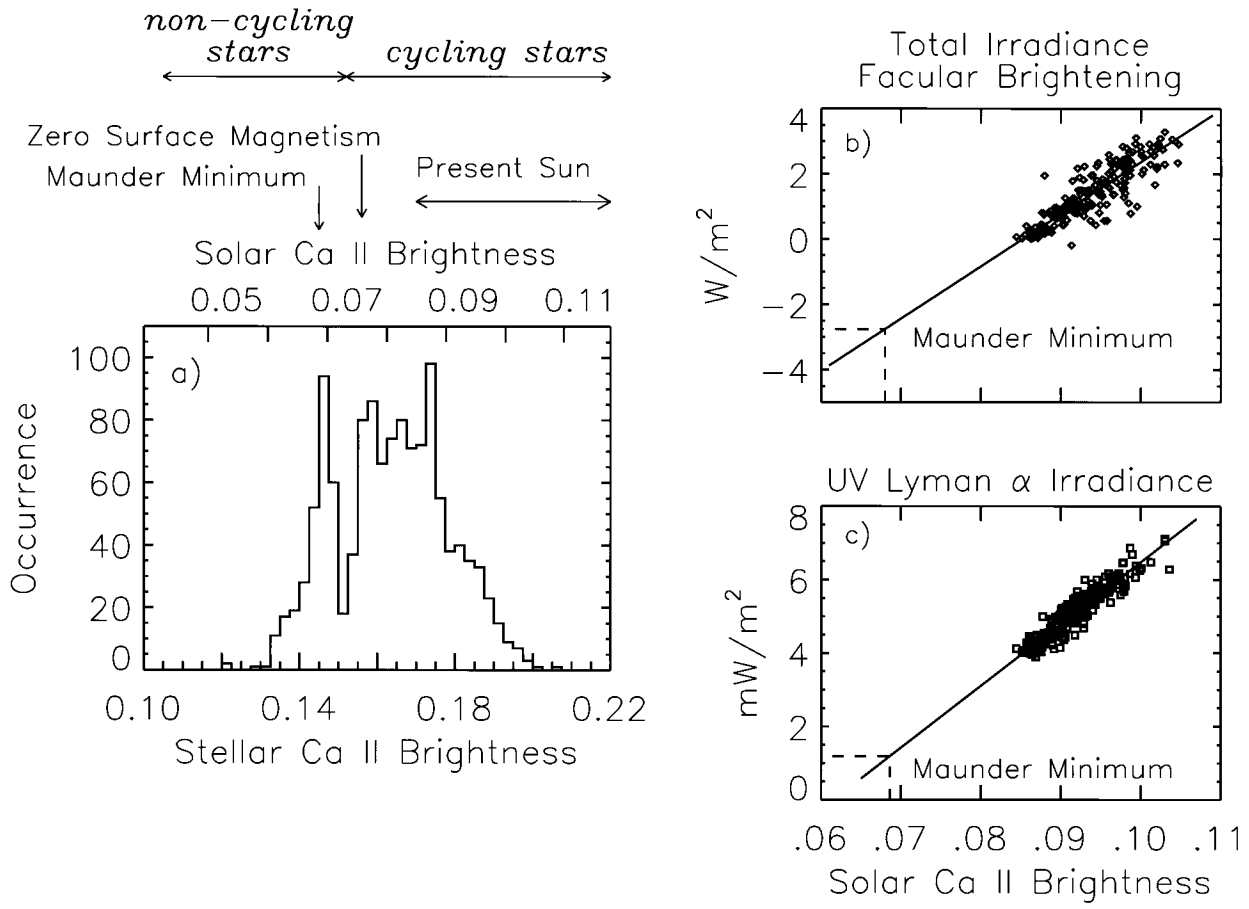

FIG. 12. Identified in the distribution of Ca II emission from solarlike stars shown in (a) is the range of Ca II emission for the present sun, which corresponds roughly to emission levels seen only in the brightest one-third of the stellar sample. The conversion between solar Ca emission (upper-abscissa label) and stellar Ca emission (lower-abscissa label) determined by White et al. (1992) allows quantitative comparison of the solar and stellar data. Whereas those stars that exhibit levels of brightness comparable to that of the present-day sun typically also exhibit activity cycles, stars with no apparent cycles are less bright. Shown on the right in (b) is a correlation between solar Ca emission and total irradiance facular brightening (determined by correcting the measured total irradiance for sunspot blocking effects), and on the right in (c) is a correlation between solar Ca emission and UV Lyman α emission (from Lean et al. 1992; Lean et al. 1995a). Scenarios whereby solar Ca emission is reduced below its contemporary range to the flux levels expected for zero surface magnetism and for the Maunder Minimum are indicated in the stellar distribution. The sun's Ca II emission during the Maunder Minimum is speculated to correspond to levels typical of noncycling stars, which then permits estimates of total and UV irradiance using the scatterplots on the right.

UV fluxes also correlate highly (White et al. 1990). Extending the linear relationship between residual total irradiance and solar Ca emission demonstrated in Fig. 12 to the lower solar Ca values inferred from stellar monitoring for noncycling stars predicts a solar total irradiance reduction of 0.24% during the Maunder Minimum relative to present-day mean levels (Lean et al. 1992). Accompanying reductions in solar UV irradiance may have exceeded (by about a factor of 2) the 11-yr cycle amplitudes of 3% at 250 nm and 7% at 200 nm (Lean et al. 1995a). The proposed mechanism is depletion of the bright facular network that normally covers the sun, even during times of present-day minima of the 11-yr cycle, and an additional reduction in the emission from the nonnetwork regions to values presently seen in only the 15% darkest regions on the solar disk (White et al. 1992). Other studies also indicate solar irradiance reductions during the Maunder Minimum from 0.2% to 0.6% below present-day values (Hoyt and Schatten 1993; Nesme-Ribes et al. 1993; Zhang et al. 1994). Independent observations of apparent luminosity changes in sunlike stars likewise estimate that larger irradiance changes are possible than evident in the present day solar monitoring database—exceeding by factors of 2 to 5 the 0.1% 11-yr solar total irradiance cycle (Lockwood et al. 1992).

The reconstruction of solar total irradiance over the past four centuries shown in Fig. 13 assumes a 0.24% solar irradiance reduction during the seventeen century relative to present-day levels. In contrast to the irradiance reconstruction shown in Fig. 10, which accounts only for the 11-yr irradiance cycle, the reconstruction in Fig. 13 combines separately determined 11-yr and longer term variability components (Lean et al. 1995b).

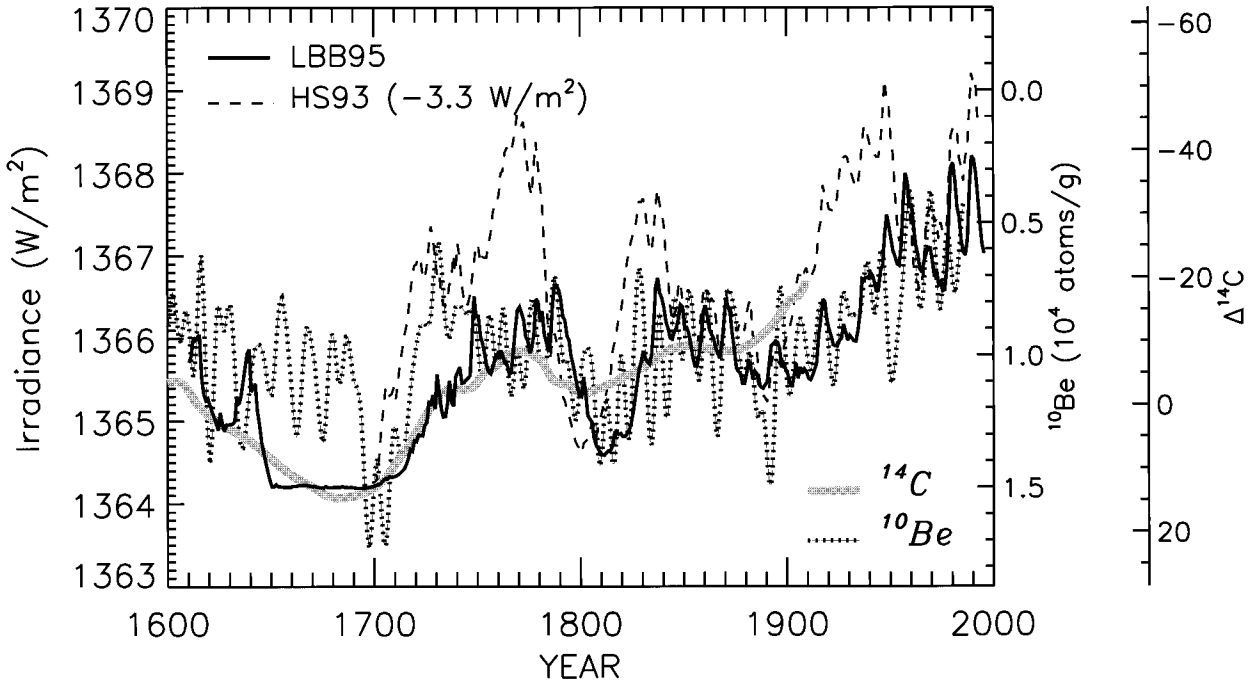

FIG. 13. Shown is a reconstruction of solar total irradiance (solid line) that includes a separately determined 11-yr activity cycle and a longer-term component based on the average amplitude of each sunspot cycle (LBB95; Lean et al. 1995b). This irradiance reconstruction is compared with ^{10}Be (small blocks) and ^{14}C (thick gray line) cosmogenic isotope records (Stuiver and Reimer 1993; Beer et al. 1994) and with the Hoyt and Schatten (1993 HS93); irradiance reconstruction (dashed line) in which longer-term changes are based on the length of the 11-yr solar activity cycle (rather than on the average amplitude).

After 1874, the total irradiance cycles are those shown in Fig. 10; prior to 1874 (when the Greenwhich data needed to calculate sunspot darkening were not recorded) the 11-yr cycle is reconstructed using directly correlated yearly mean total irradiance and group sunspot numbers (see, e.g., Schatten and Orosz 1990). Following the demonstration by Foukal and Lean (1990) that facular brightening tracks the monthly mean sunspot number throughout the 11-yr cycle, on longer timescales the network facular emission is assumed to likewise track the overall level of solar activity, and the shape of these changes is specified by the average amplitude of the group sunspot number (Hoyt et al. 1994) in each cycle. This longer-term component is scaled to cause an increase of approximately 0.2% in total solar irradiance and 0.97% in UV (200–300 nm) irradiance from the Maunder Minimum to the present. Including the 11-yr activity cycle, overall variability from the Maunder Minimum to the present-day mean is thus constrained to agree with a total solar irradiance change of 0.24% (Lean et al. 1992).

The total irradiance reconstruction in Fig. 13 that includes both an 11-yr cycle and a longer-term variability component tracks independent records of solar activity levels inferred from ^{14}C and ^{10}Be cosmogenic isotopes (Stuiver and Braziunas 1993; Beer et al. 1994). However, this reconstruction differs somewhat from that of Hoyt and Schatten (1993), which has a long-term variability component based on the length (rather than amplitude) of the activity cycle. These differences, which cannot be resolved without improved understanding of the solar origins of the variations, reflect the large uncertainties in reconstructing historical solar irradiances from a limited solar monitoring database, with only rudimentary knowledge of the pertinent physical processes.

3. Statistical sun–climate connections

Similarities among various climate and solar activity records (e.g., Figs. 2 and 4) suggest that climate variability in the recent Holocene may be partly attributable to the variable sun. Some climate records have periodicities at 11 and 22 yr that are common also in solar activity proxies. Other climate records appear to correlate well with long-term solar activity on decadal to century timescales. Some of these relationships are summarized below. That not all climate time series exhibit this anecdotal evidence for solar forcing is usually interpreted as evidence to reject the hypothesis of a sun–climate connection, leading to present ambiguity about the physical reality of the effect. Resolving this ambiguity requires proper identification of physical mechanisms to explain the cycles and correlations.

TABLE 2. Some periods other than the 2.2-yr QBO present in climate records (adapted from Burroughs 1992).

Source	Period (yr)
Global surface temperature (Mann and Park 1994)	3–5, 10, 27
Central England temperature (Mason 1976)	3.1, 5.2, 7.5, 14.5, 23, 76
U.S. east coast temperature (Karl and Riebsame 1984)	4.5, 9, 20
Global marine air temperature (Newell et al. 1989)	22
U.S. drought (Mitchell et al. 1979)	22
Beijing rainfall (Hamseed et al. 1983)	9.9, 18.7, 56, 84, 126
U.S. rainfall (Curie and O'Brien 1988)	11, 18.6
Nile floods (Hameed 1984)	18.4, 22, 77
South American rainfall	3.8, 7, 20
African rainfall (Seleshi et al. 1994)	3.5, 10–12, 18
North Atlantic pressure (Kelly 1977)	3.4, 5, 11
Southern Oscillation	3, 3.8, 6, 10–12, 22, 34
North American forest fires (Auclair 1992)	11
Atlantic tropical cyclones (Cohen and Sweester 1979)	8, 9.3, 11.3, 14.8, 22, 51.3, 133
Tropical corals (Dunbar et al. 1994)	3.3, 4.6, 6, 8, 11, 17

a. Cycles

Climate records exhibit a range of periods, some of which are listed in Table 2 (adapted from Burroughs 1992), none of which reflect truly deterministic climate cycles. Presumably arising from nonstationary processes, climate periodicities exhibit variable phase and amplitude, appearing only in some climate proxy records, in certain geographical regions, in some epochs, and not always in phase with their surmised forcing mechanisms. Burroughs (1992) (see also Hoyt and Schatten 1997) interprets the high occurrence of the cycles listed in Table 2 simply as recognition of potential climate variability modes. Recent analyses of the global surface temperature record since 1860 lends some support for this interpretation by identifying climate cycles in the range 2–8 yr and 11–12 yr with confidence limits in excess of 90% (Mann and Park 1994). However, a robust statistical description of climate variability and of the significance of all of the peaks in Table 2, especially those with longer periods, has proven elusive, even when potential physical mechanisms are identified. Rather, processes internal to the climate system likely cause a ''substantial share of the variability of climate'' (Mitchell 1976) with external climate forcing processes contributing additional variability to this stochastic background.

Periodicities in the range 2–7 yr are attributed with some confidence to internal oscillations in the coupled ocean–atmosphere system; those at 2–3 yr are connected to the quasi-biennial oscillation (QBO) in tropical stratospheric winds, and those from 3–7 yr to the El Niño–Southern Oscillation (ENSO) (see, e.g., Mann and Park 1994; Dunbar et al. 1994). Although decadal and multidecadal periods are common in climate time series, their physical origins are difficult to specify, partly because of the paucity of global coverage by long-term climate records with high (annual) resolution. Periods near 18 and 34 yr are often connected to lunar forcing. Since sunspot numbers exhibit a pronounced 11-yr cycle, periods near 11 and 22 yr are tentatively connected with solar variability, often for lack of another plausible mechanism. But the transitory nature of this period and its absence in some climate records lead Pittock (1979) to dismiss the implied sun–climate connection as unconvincing. Recognition that the solar radiative output varies does imply a potential mechanism for excitation of these periods by solar forcing, a scenario that was harder to formulate when solar irradiance was assumed to be constant. Alternative mechanisms are also postulated for the decadal periodicities, in particular an internal oscillation of the climate system that is present in some climate model simulations in the absence of external forcing (James and James 1989; Mehta and Delworth 1995).

As noted above, spectral analysis of the ^{14}C record indicates apparent fluctuations in periods ranging from less than 100 to several thousand years, including the 88-yr (Gleisberg) cycle, and ~210 and ~2300 yr cycles. Hints of these cycles have also been identified in the climate record, for example, the 2500-yr cycle in marine, glacier, and polar ice core records (Denton and Karlen 1973; Dansgaard et al. 1984; Pestiaux et al. 1987; Wigley and Kelly 1990), and the 88- and 200-yr cycles in varved sediments (Halfman and Johnson 1988; Peterson et al. 1991; Anderson 1992). Whether these are truly periodic in nature is doubtful, but they are indicative of a general coincidence of apparently increased ^{14}C production (i.e., lower solar activity) and colder temperatures (de Vries 1958; Eddy 1976), with the Maunder Minimum–Little Ice Age being the most recent example.

b. Correlations

Episodes of correlated climate and solar variability occur throughout the Holocene, on timescales ranging from subdecadal to multicentennial.

Tropospheric temperatures during the past few decades appear to be about 0.5° to 1.5°C warmer during times of cycle maxima, notably in the midlatitude Western Hemisphere (Labitzke and van Loon 1993a,b). A 0.15°C increase in land-surface temperatures from 1986 to 1990 has been attributed to increasing solar irradiance from cycle 22 minimum to maximum activity (Ardanuy et al. 1992). Sea surface temperatures bandpassed to isolate the decadal component of their variability exhibit changes of the order of 0.1°C that are highly correlated (correlation >0.9) with the sun's 11-yr activity cycle in

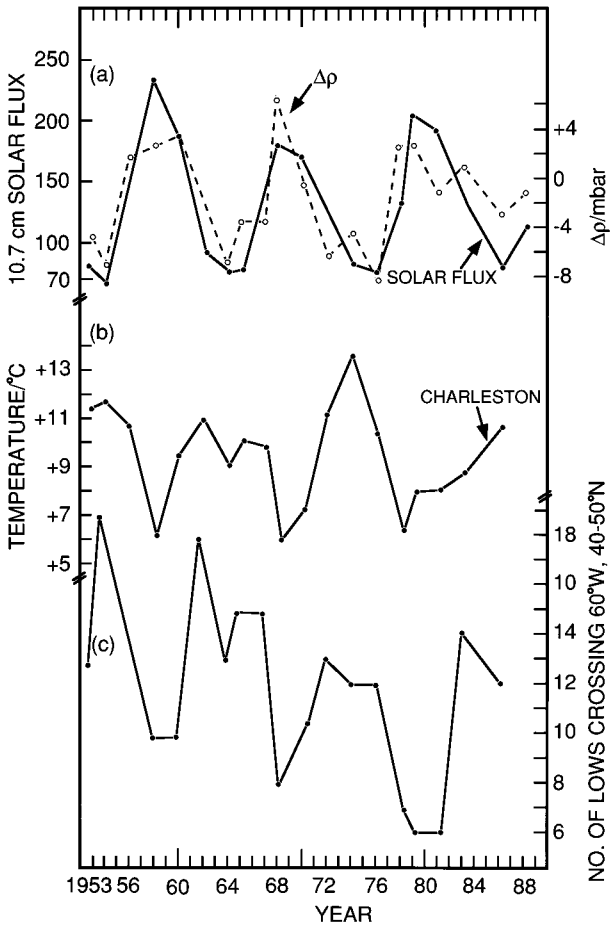

FIG. 14. Compared in (a) are the 10.7-cm solar flux and the atmospheric pressure difference [(70°N, 100°W) minus (20°N, 60°W)] in the ''west'' years of the equatorial stratosphere quasi-biennial oscillation (QBO) in Jan–Feb. The changes in the differences between the land (100°W) and sea (60°W) pressures are correlated with the 11-yr solar activity cycle. Shown in (b) is the surface air temperature at Charleston, South Carolina, during Jan–Feb in QBO west years and in (c) the number of lows crossing the 60th meridian west between the latitudes of 40°N and 50°N. From Labitzke and van Loon (1990).

the past four decades (White et al. 1997). Coral records of $\delta^{18}O$ infer that the relationship between the sun's 11-yr cycle and sea surface temperatures extends over the past 400 yr (Dunbar et al. 1994). Furthermore, solar-related sea surface temperature changes may initiate regional precipitation fluctuations (Perry 1994). High resolution ice core records provide further evidence for apparent correlations of climate parameters with the sun's 11-yr cycle both at midlatitude high-altitude sites, (Thompson et al. 1993) and in the high-latitude Greenland GISP2 (Grootes and Stuivers 1997) ice core. Furthermore, correlations of climate parameters with the 11-yr cycle may be enhanced significantly when the climate data are sorted according to the phase of the QBO, as illustrated in Fig. 14 (Tinsley 1988; Barnett 1989; Labitzke and van Loon 1990).

Figure 4 demonstrates the correlation of globally and hemispherically averaged surface temperatures and solar activity over multidecadal timescales in the past 140 yr, and the data in Fig. 15 (Eddy 1976, 1977) extend this apparent sun–climate correction to the past few centuries, using solar variability inferred from cosmogenic isotopes. During the past 9000 yr, climate minima identified in a composite of glacial advance and retreat records correspond to six out of the seven lowest levels of solar activity represented by peaks in the ^{14}C isotope data (Wigley and Kelly 1990).

Despite their ubiquity, correlations among climate and solar parameters remain tenuous paradigms for assessing the range of natural variability possible for the earth's climate, against which to gauge the extent of natural versus anthropogenic variability in the recent century. Neither climate nor solar variability are sufficiently well defined, either spatially or temporally, nor their causes adequately understood, to verify that the correlations really arise from climate forcing by changing solar radiation rather than from statistical coincidence (Baldwin and Dunkerton 1989; Salby and Shea 1991). In the recent Holocene, for example, the correlations arise, for the most part, from the coincidence of the Little Ice Age from roughly 1450 to 1850 with the Spörer and Maunder minima in solar activity and of the thirteenth century Medieval Warm Period with the Medieval Maximum of solar activity. Yet neither the Little Ice Age (Bradley and Jones 1993) nor the Medieval Warm Period (Hughes and Diaz 1994) is a quantitatively well-characterized climatic episode; nor are these events prominent in all climate records (Briffa et al. 1990).

Inferences from sun–climate correlation studies can depend critically on the type and length of the climate and solar variability records chosen for the study. Although in the past 130 yr the Hoyt and Schatten (1993) irradiance reconstruction correlates well with NH surface temperatures (correlation of 0.8), from 1700 to 1990 its correlation with the Bradley and Jones (1993) NH temperature data drops to 0.5 (Crowley and Kim 1995). A higher correlation of 0.7 is obtained with the Bradley and Jones (1993) NH temperature record using the irradiance reconstruction in Fig. 13 in which the longer-term component is based on the amplitude, rather than length of the 11-yr cycle (Lean et al. 1995b). Yet when annual sunspot numbers (SSN) (which lack the longer-term component evident in cosmogenic isotopes and the irradiance reconstructions, Fig. 13) are used as a proxy for solar activity ''the influence of SSN on global temperatures is found to be negligible'' (Visser and Molenaar 1995).

Changing strengths of sun–climate correlations in different epochs may reflect real changes in the relative amplitudes of the various climate forcings, for example, prior to and during the industrial epoch. This is demonstrated in Table 3 by the correlation of the decadal means during the past four centuries of data similar to those in Fig. 2 (the sun's total irradiance, the volcanic dust veil index, CO_2 concentrations, and surface tem-

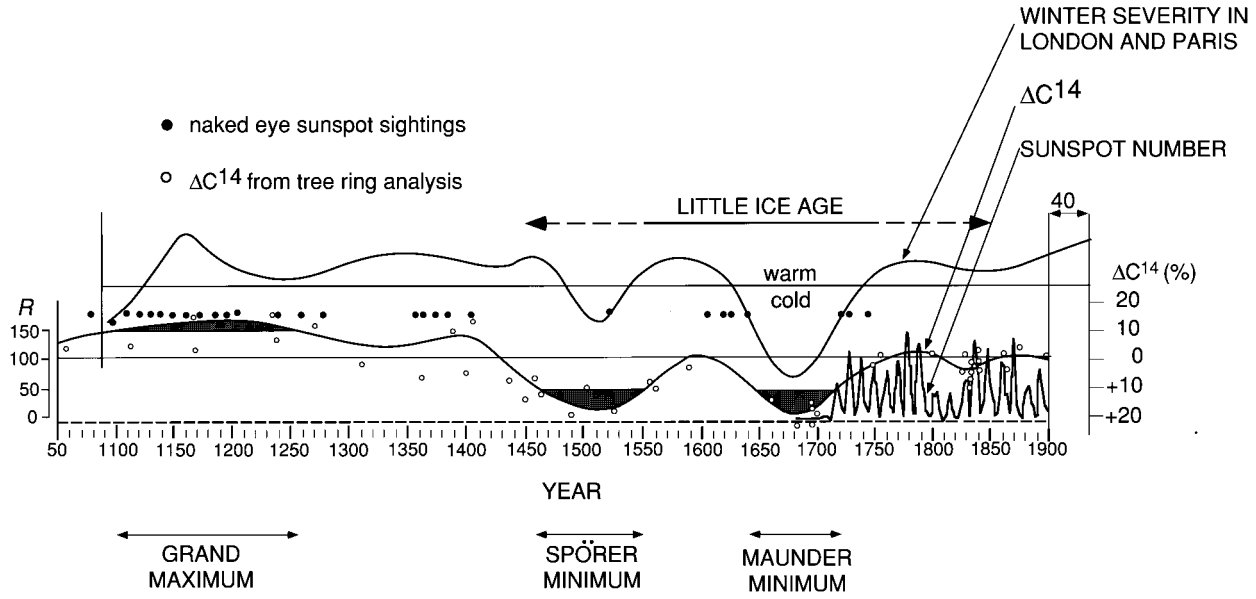

FIG. 15. Shown is the relationship between winter severity in Paris and London (top curve) and long-term solar activity variations (bottom curve). The shaded portions of this curve denote the times of the Spörer and Maunder minima in sunspot activity. The dark circles indicate naked-eye sunspot observations. Details of the solar activity variation since 1700 are indicated in the bottom curve by the sunspot number data. The winter severity index has been shifted 40 yr to the right to allow for cosmic ray-produced ^{14}C assimilation into tree rings. From Eddy (1976, 1977).

perature anomalies). From 1610 to 1800 the correlation of reconstructed solar irradiance and NH temperature is 0.86, whereas the correlation of NH dust veil index with surface temperature is −0.005, implying a predominant solar influence in this preindustrial period. From 1800 to 2000 the correlation of surface temperature and the NH dust veil index is stronger (−0.51), reflecting extended volcanic activity in the nineteen century. Since 1800, both greenhouse gas concentrations and solar activity have steadily increased (although at different rates) whereas volcanic activity declined in the twentieth century relative to the nineteenth century. From 1800 to 2000, surface temperatures correlate more strongly with CO_2 levels than with reconstructed solar irradiance, in contrast to the prior two preindustrial centuries.

Contrary to the implications of Table 3 that solar forcing may account for a significant fraction of recent climate variability, Robock (1979) suggests that in fact volcanic dust forcing produces the best simulation of climate change in the past 400 yr. Furthermore, his study found no evidence for a solar influence on climate during the Maunder Minimum, in part because the reconstructed temperature time series used was less cold during that epoch than is the Bradley and Jones (1993) reconstruction (e.g., Fig. 1). Other studies that utilize the Crête (Greenland) ice core acidity record have likewise inferred a strong volcanism signal in climate variations of the last 1400 yr, a correspondence that, however, is less impressive when background acidity levels of presumably nonvolcanic origin are removed (Crowley et al. 1993). Whereas clusters of intense volcanism might occasionally cause a decadal-scale climate excursion, Crowley and Kim (1995) attribute 30% to 55% of climate variability on decadal–centennial timescales to solar variability.

Assuming that climate forcing by changing solar ra-

TABLE 3. Correlation of decadal means of solar variability, the volcanic dust veil index, and CO_2 greenhouse gas concentrations with NH surface temperature anomalies, composing the Bradley and Jones (1993) NH summer data from 1610 to 1850, scaled to Houghton et al. (1992) NH annual data, and the IPCC NH data since then, as shown in Fig. 1.

	Correlation coefficient (with NH surface temperature)	
Climate forcing parameter	1610–1800 19 points	1800–2000 20 points
Sun: reconstructed total irradiance (Lean et al. 1995b)	0.86	0.77
reconstructed total irradiance (Hoyt and Schatten 1993)	–	0.69
Volcanic dust veil index: global	−0.12	−0.57
NH	−0.005	−0.51
SH	−0.23	−0.55
Greenhouse gases: CO_2	0.70	0.86

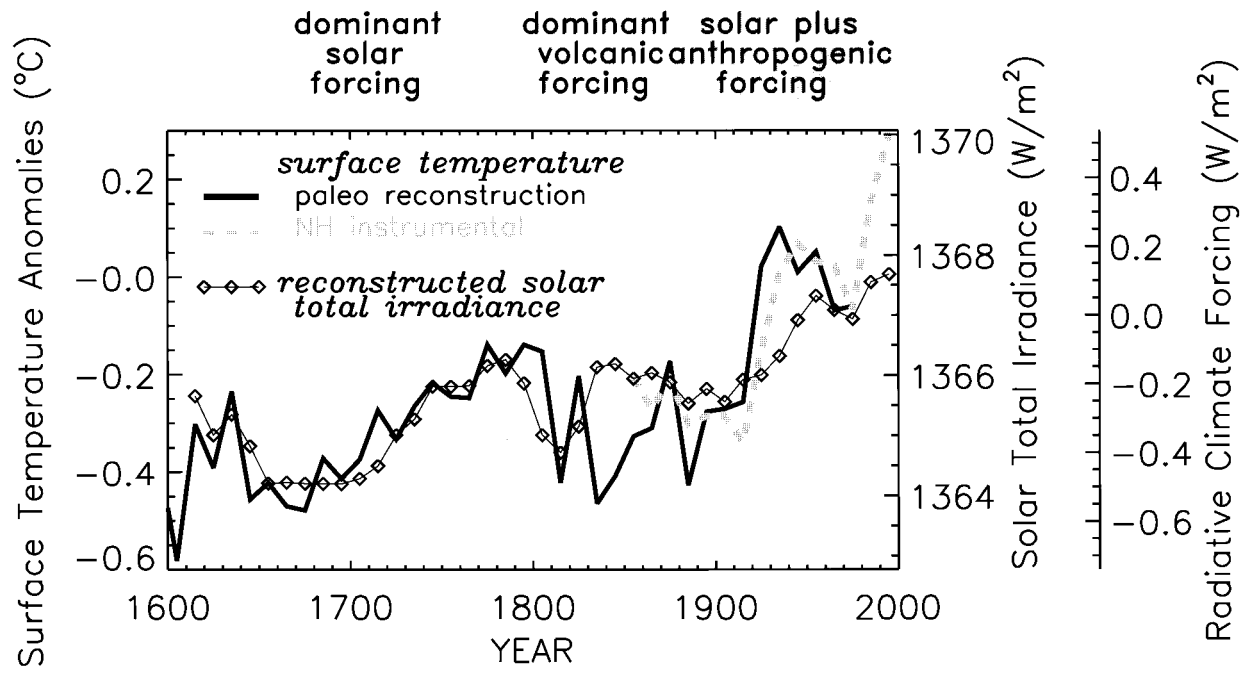

FIG. 16. Compared are decadally average values of the Lean et al. (1995b) reconstructed solar total irradiance (diamonds) from Fig. 13 and NH summer temperature anomalies from 1610 to the present (similar annually averaged data are shown in Fig. 2). The solid line is the Bradley and Jones (1993) NH summer surface temperature reconstruction from paleoclimate data (primarily tree rings), scaled to match the NH instrumental data (Houghton et al. 1992) (dashed line) during the overlap period as given in Fig. 1.

diation S is responsible for the surface temperature variability ΔT from 1610 to 1800, a linear relationship of $\Delta T = -168.666 + 0.1233 \times S$ is deduced from the preindustrial data (update from Lean et al. 1995b) and extended in Fig. 16 to the industrial period from 1800 to 2000. According to the simple preindustrial parameterization, surface temperature changes arising from changing solar radiation may have contributed about half of the 0.55°C warming since 1900, but since 1970 no more than one-third of the 0.35°C warming is attributable to the variable sun.

4. Simulations of climate response to changing solar radiation

Until physical causal mechanisms are identified to explain the apparent associations of solar and climate variability it will be difficult to prove or disprove that these associations arise from climate forcing by changing solar radiation, rather than from other mechanisms such as internal oscillations, or simply from statistical perturbations from a postiori choices. Uncovering potential mechanisms for decadal and centennial climate change requires improved specification of the climate system's response to individual and combined radiative forcings, and simulations of the expected influence of realistic solar radiation changes over these timescales.

a. Equilibrium simulations

Although the climate system response to radiative forcing likely depends on the strength, history, geographical distribution, and attitudinal localization of the specific forcing, these relationships are poorly quantified. In practical applications, climate sensitivity is specified to be in the range $\kappa = 0.3°$–1°C per W m^{-2}, such that an equilibrium temperature change $\Delta T = \kappa \Delta F$ (°C) results from a radiative forcing of ΔF (W m^{-2}). Changes in solar radiation ΔS cause radiative forcing $\Delta F_s = \Delta S \times 0.7/4$ where the factor 0.7 accounts for the reflection back to space of a portion of the incident solar energy (the albedo) and the factor 4 is the spherical average. With this simple prescription, an equilibrium surface temperature change in the range 0.07°–0.24°C is estimated to result from the total irradiance change in solar cycle 21 ($\Delta S = 1.1$ W m^{-2}, Fig. 10) (Wigley and Raper 1990) and a larger temperature change in the range 0.17 to 0.57°C is estimated for the speculated longer-term irradiance change of 0.24% ($\Delta S = 3.3$ W m^{-2}) from the seventeenth century to the present. Consistent with this an equilibrium simulation by the Goddard Institute for Space Studies (GISS) general circulation model (Hansen et al. 1983)—whose sensitivity is in the range 0.7°–1°C per W m^{-2}—estimates a global surface temperature decrease of 0.47°C for a 0.25% solar irradiance decrease (Rind and Overpeck 1993). An additional complicating feature is that κ may be different for decadal

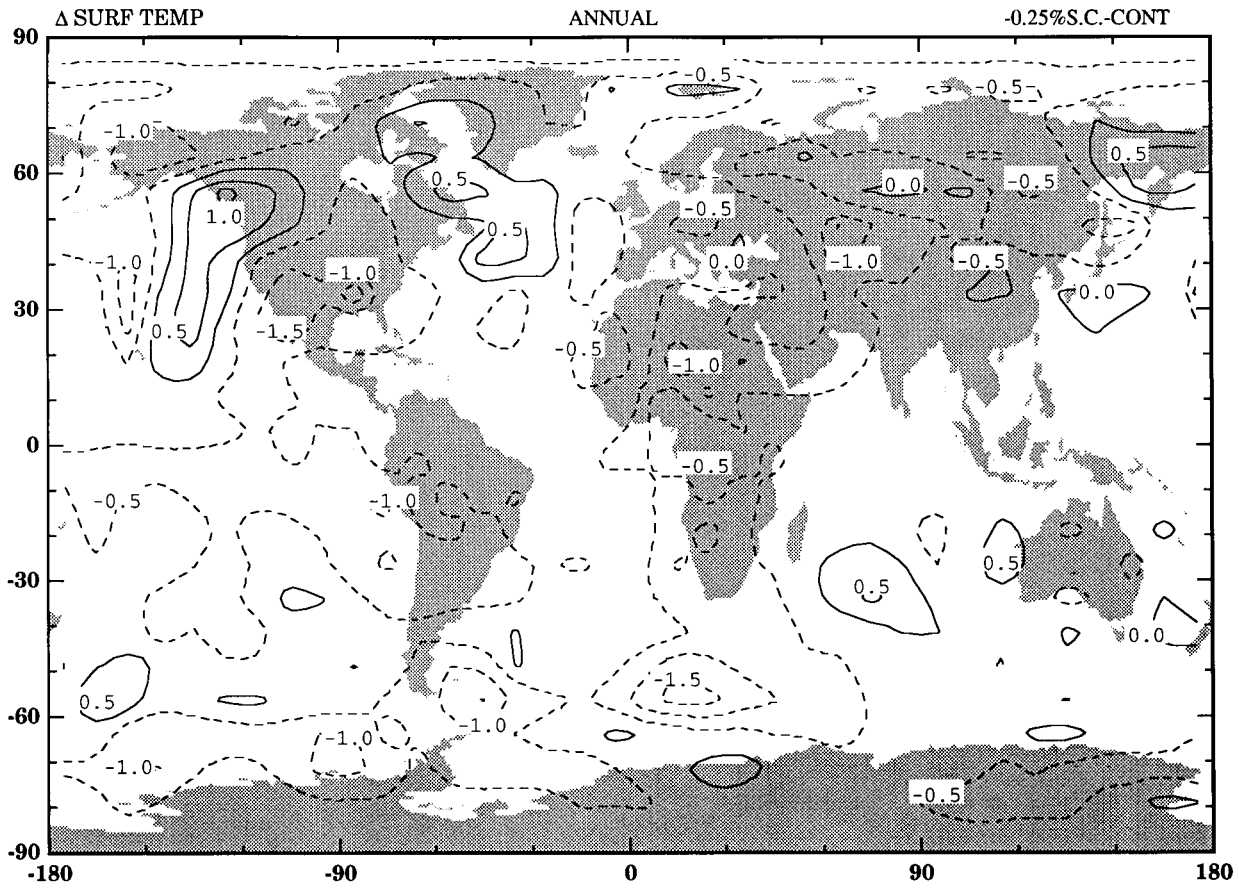

FIG. 17. Calculations by the GISS/GCM of the annually averaged terrestrial temperature response to a reduction of 0.25% in total solar irradiance. It is possible that a reduction of this magnitude occurred during the Maunder Minimum in solar activity (Fig. 1), which lasted from approximately 1645 to 1715 and coincided with the coldest temperatures of the Little Ice Age (Fig. 15). Notice that with this magnitude of solar irradiance reduction, the GISS/GCM predicts that not every locale experiences cooling, as advective changes can dominate the radiative cooling (from Rind and Overpeck 1993).

and century scale perturbations, with the longer-term forcing exciting more oceanic response and system feedbacks (Hansen et al. 1985).

An important feature of the GISS simulation shown in Fig. 17, however, is that although a 0.25% reduction in solar irradiance causes 0.47°C global cooling, some geographical locations cool and others warm by more than 1°C as a result of dynamical circulation patterns driven by the differential heating of the land and the oceans (Fig. 18, top panel). Although many of the changes in Fig. 17 simulated by the GISS model were of the same order as the model standard deviation, especially at high latitudes, the geographical patterns were verified to some extent by comparing two different time slices of the simulation after the model had reached equilibrium (Rind and Overpeck 1993). The model was integrated for 60 model years using a version that allowed sea surface temperatures to change while keeping ocean heat transports specified at current values (Hansen et al. 1984). The differences in surface air temperatures shown in Fig. 17 were estimated during years 36–45 of the experiment, and a similar time period for the current climate control run, and are generally similar to estimates from later years.

Equilibrium simulations of climate response to changing solar radiation using the Laboratoire de Meteorologie Dynamique (LMD) atmospheric GCM estimate surface temperature reductions of 1.5°C for the seventeenth century Maunder Minimum, for a 0.4% irradiance decrease—a 320% larger temperature reduction than the GISS simulations for a 60% larger irradiance change—with minimal geographic inhomogeneity (Nesme-Ribes et al. 1993). Perhaps the factor of 3 larger cooling, a result of the high sensitivity of the LMD model, was sufficient to overcome the regional advective patterns initiated by the differential land–ocean heating for less cooling; different geographical locations may exhibit quite different responses to small changes in solar radiative forcing, depending on the magnitude of the forcing. As a result of reduced solar irradiance in the seventeenth century, the GISS and LMD simulations also predicted changes in other climate parameters, including evaporation minus precipitation shown in Fig. 18 (bottom panel).

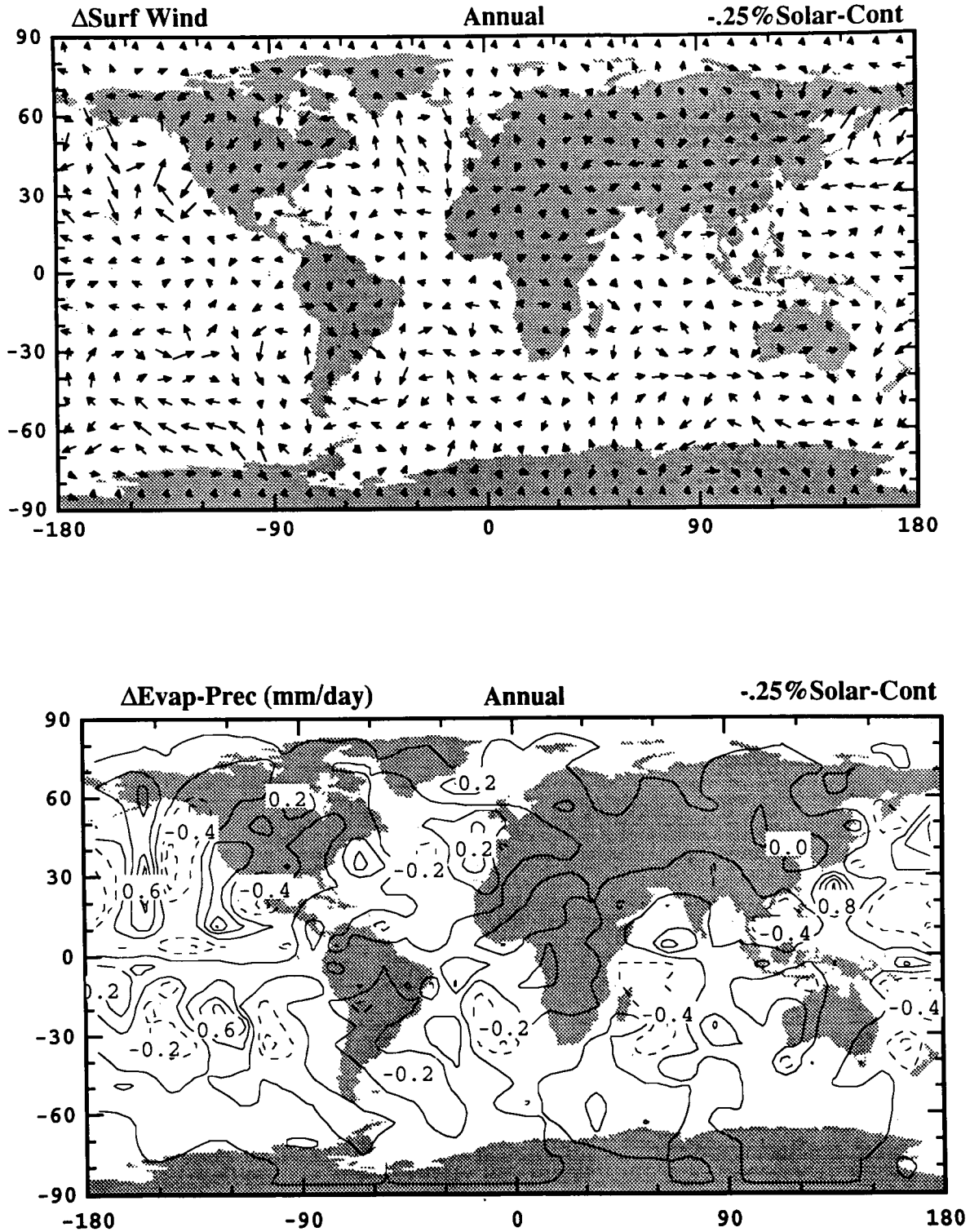

FIG. 18. Shown are annual average changes in the GISS/GCM surface winds (top panel) and evaporation minus precipitation (bottom panel) resulting from a spectrally flat solar total radiative output decrease of 0.25%, accompanying the surface temperature changes in Fig. 17 (Rind and Overpeck 1993).

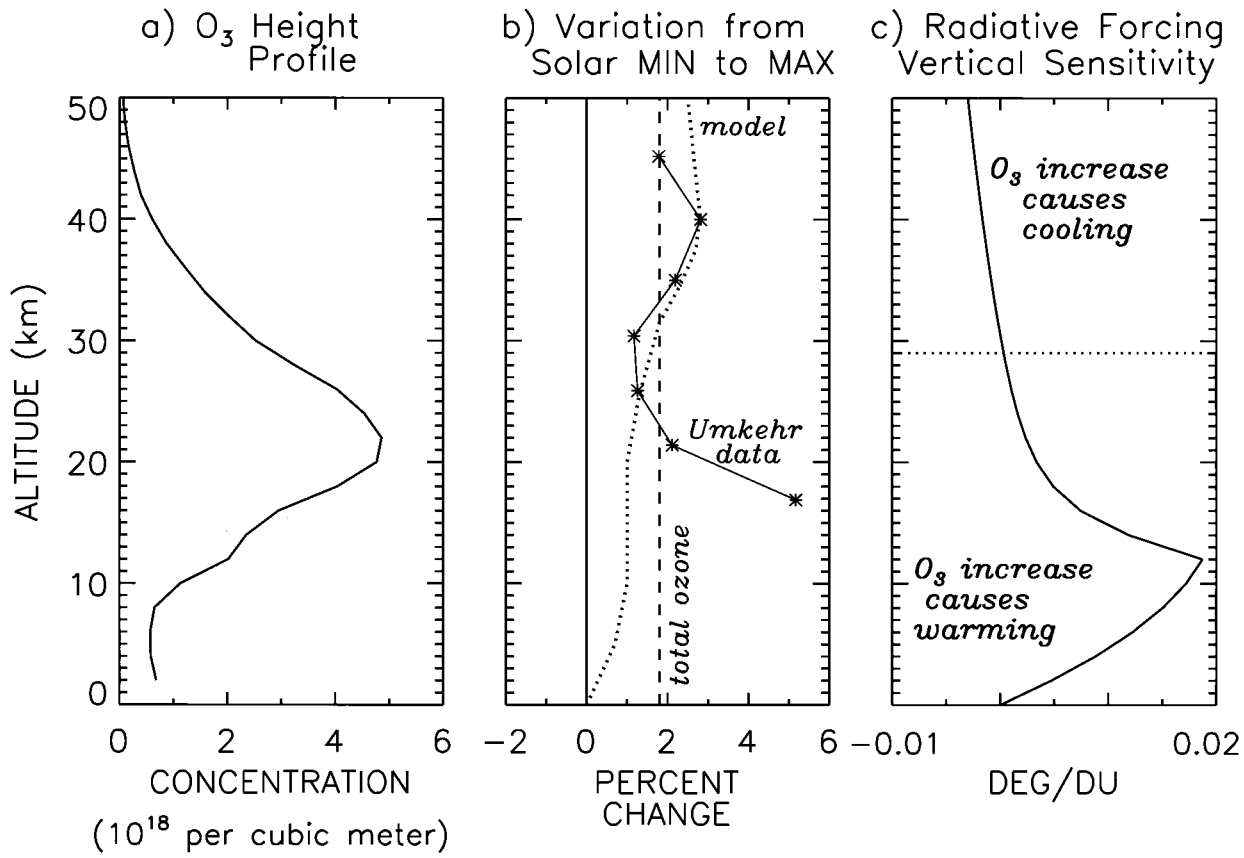

FIG. 19. The *U.S. Standard Atmosphere*, 1976 atmospheric ozone profile is shown in (a) and estimated solar cycle ozone changes are shown in (b) based on a model simulation by Wuebbles et al. (1991) and a trend analysis of Umkehr data by Reinsel et al. (1994). Shown in (c) is a one-dimensional radiative–convective equilibrium calculation of the vertical sensitivity of the radiative forcing of climate by changing ozone concentrations (in DEG/DU), indicating how the impact of altered ozone concentration (in Dobson units) on surface temperature (in °C) depends on the altitude profile of the ozone changes (Lacis et al. 1990).

Simulations of the climate response to changing solar radiation with energy balance models or GCMs typically utilize only the total changes in solar radiative output and ignore the spectral dependence of this variability (Pollack et al. 1979). A related omission in these simulations is that solar modulation of the ozone layer and the middle atmosphere are not accounted for, thus neglecting possible climate forcing by radiative and dynamical coupling of the middle atmosphere with the troposphere (Haigh 1994, 1996). Both total column ozone amount and the altitude distribution are known to be affected by solar UV radiation at wavelengths less than 300 nm that is absorbed in the earth's middle atmosphere (see Fig. 5) (Hood and McCormack 1992; Reinsel et al. 1994; Chandra and McPeters 1994; Hood 1997; see also NRC 1994).

Ozone concentration changes may, as shown in Fig. 19, either cool or warm the earth's surface depending on the altitude of the changes as both short wave absorption and infrared forcing are affected (Lacis et al. 1990; Schwarzkopf and Ramaswamy 1993; Haigh 1996). Stratospheric variations in response to changing solar UV radiation and ozone, also shown in Fig. 19, may affect the troposphere and climate by altering tropospheric dynamics, as suggested both by observations and modeling studies. Some results of tropospheric variations associated with the quasi-biennial oscillation and UV variations from the studies of Labitzke and van Loon are given in Fig. 14. A recent set of modeling studies found that UV variations imparted to a global climate–middle atmosphere model in conjunction with the QBO did have significant effects on both the stratosphere and troposphere (Balachandran and Rind 1995; Rind and Balachandran 1995). The mechanisms involved are summarized in Fig. 20. The QBO alters the meridional gradient of the zonal wind in the lower stratosphere, and UV variations alter the vertical gradient of the zonal wind. Both change the refraction properties of planetary waves in the stratosphere, resulting in dynamically induced warm–cool regions in the stratosphere. This thermal response then alters the vertical stability of the troposphere–stratosphere system and in the model affects tropospheric planetary wave generation, especially for the longest planetary waves.

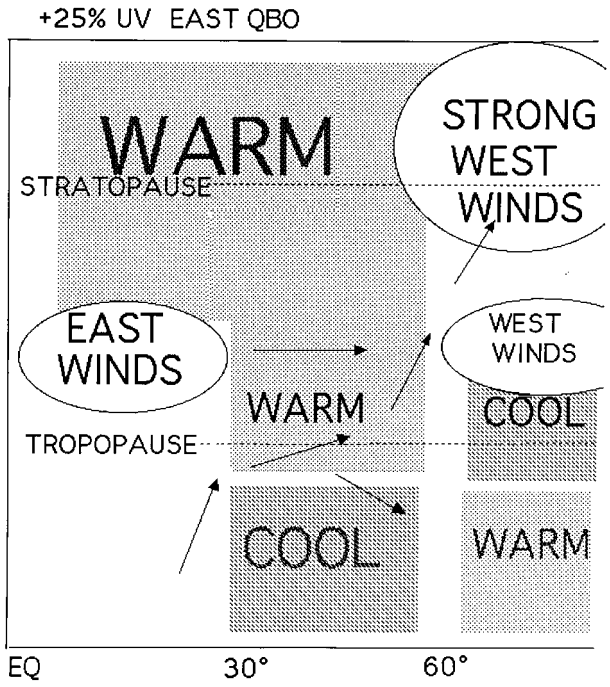

FIG. 20. Shown is a schematic of middle atmosphere–troposphere response pathways to changes in the east phase of the QBO with increased solar UV radiation. Tropical east winds lead to greater poleward propagation of planetary wave energy (arrows) in the lower stratosphere, producing warming at midlatitudes. The increased UV radiation produces general warming at low- to midlatitudes, and increased west winds at higher levels in the extratropics. This larger vertical shear of the zonal winds is associated with greater upward planetary wave energy propagation, taking energy out of the polar lower stratosphere, which thus cools. The extratropical tropospheric response is opposite to that of the lower stratosphere, due to the effects of changes in vertical stability on eddy energy and high cloud cover (Rind and Balachandran 1995).

In conjunction with altered planetary wave generation and propagation (hence weather), changes in cloud cover and atmospheric energy transport occur, altering the mean climate state and producing surface air temperature change. Shown in Fig. 21 is the change in surface air temperature between +5% UV and −5% UV radiation in the QBO west phase (top panel) and east phase (middle panel), averaged over 10 Januaries in the model. Distinctive warm and cool regions arise, which vary between the west and east QBO phase (Fig. 21, bottom panel). The model results are somewhat similar to observations, and imply that the sun's UV radiative output changes may affect surface temperatures by acting through the stratosphere. When averaged over the solar cycle there is no guarantee that these perturbations will cancel, in contrast to assumptions that since the 11-yr activity forcing is cyclic, any effect is assumed to give a net zero forcing over each cycle. This prospective mechanism emphasizes that the potential complexity of the climate system should not be underestimated, and that caution is needed in translating the magnitude of climate forcing into a climate response (Rind and Balachandran 1995).

b. Time-dependent simulations

Equilibrium temperatures are only realized for climate forcings that persist over sufficiently long times relative to the time response of the climate system. Time-dependent simulations using energy balance models suggest that oceanic thermal inertia dampens the 11-yr cyclic solar forcing by roughly 80%: the expected solar-related surface temperature changes are in the range 0.02°–0.03°C, perhaps too small to be detected in the climate record (Wigley and Raper 1990) except with sophisticated statistical tools (North and Kim 1995; Stevens and North 1996). In response to the longer-term 0.36% irradiance increase since 1700 estimated by the Hoyt and Schatten (1993) reconstruction (Fig. 13), a recent energy balance model estimates surface temperature change in the range 0.2°C–0.3°C (Crowley and Kim 1995). Attempts by energy balance models to simulate climate change in the past 140 yr provide circumstantial evidence for forcing by greenhouse gases, sulfate aerosol, and solar variability, with greenhouse gas forcing dominant in the past century. Unambiguous conclusions are prevented in part by uncertainties in the amplitudes of the aerosol and solar irradiance changes (Kelly and Wigley 1992; Schlesinger and Ramankutty 1992).

Very recently, we have used the GISS 8° × 10° GCM to simulate the time-dependent climate response to solar forcing during the past four centuries, using as input the solar irradiance reconstruction in Fig. 13 (solid line). Power near 11, 22, and 60 yr present in the solar forcing time series is ambiguous in the simulated surface temperature response, although enhanced power is evident at the longer periods. Global surface temperature changes associated with the overall 0.24% irradiance increase from the seventeenth century Maunder Minimum to the present are of the order of the equilibrium simulation (i.e., in the range 0.3°–0.5°C). Five individual time-dependent simulations and associated control runs have been performed and the results are presently being analyzed. The runs were made in conjunction with National Oceanic and Atmospheric Administration (NOAA) Climate and Global Change and Paleoclimate programs, as part of the Analysis of Rapid and Recent Climate Change (ARRCC) effort to characterize climate change and responses to natural (solar, volcanic) and anthropogenic (greenhouse gas, aerosol) forcings during the past 400 yr. Planned is a detailed analysis of time series and geographic maps of transient surface temperature, cloud cover, precipitation, and other climate parameters and comparison of the simulations with available data to better assess the reality of solar and other influences on recent climate change, both globally and regionally.

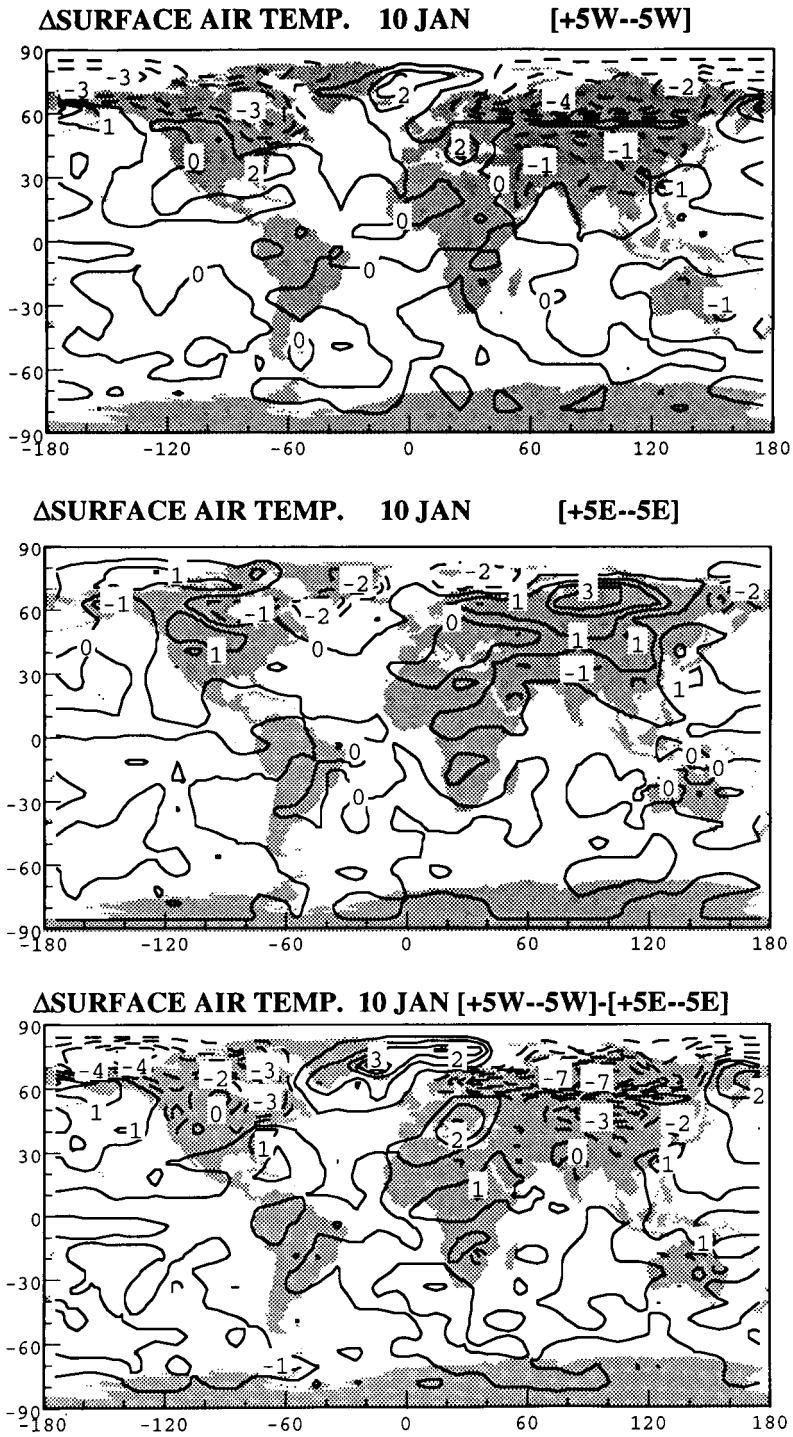

FIG. 21. Simulation by the GISS middle atmosphere GCM of the impact on surface air temperature of a ±5% change in the solar UV radiation, for both the west and east phases of the QBO. Model surface air temperature difference (°C) are averaged over 10 Januaries for (top panel) (+5W) minus (−5W), (middle panel) (+5E) minus (−5E), and (bottom panel) (+5W minus −5W) minus (+5E minus −5E) (Rind and Balachandran 1995).

5. Summary and discussion

Radiation from the sun—the earth's energy source—varies continuously at all wavelengths and on all observed timescales. A change in total radiative output of about 0.1% has been measured between the maximum and minimum of the sun's recent 11-yr activity cycle. Accompanying changes occur throughout the solar spectrum, with larger cycle amplitudes in radiation at UV wavelengths than in visible emissions. Although not measured directly, total radiative output changes of a few tenths percent are postulated to occur over centennial timescales, based on evidence from cosmogenic isotope proxies of solar activity and activity levels in sunlike stars, both of which exhibit a larger range of variability than yet evident in the present-day sun.

Response of the climate system to radiative forcing, including by the variable sun, is not yet understood with sufficient certainty to unambiguously interpret the earth's surface warming over the past 140 yr. Presently specified climate sensitivity overpredicts the magnitude, and cannot replicate the shape of the surface warming expected from radiative forcing by greenhouse gases alone. This underscores the need to quantify all other natural and anthropogenic influences, including those of less magnitude than greenhouse gases, since the assumption of similar climate response to forcings of similar magnitude may not be valid.

In the recent past, correlations between solar variability and surface temperatures rival those between surface temperatures and greenhouse gases, and there is evidence of the 11-yr solar activity cycle in a variety of climate data. Neither the amplitude of the climate response to changing solar radiation, nor its temporal or geographic character has yet been established with the certainty needed to either validate or dismiss these observed sun–climate associations. Even if putative long-term changes in solar radiation do not occur with the magnitude of the reconstructed irradiances shown in Fig. 13, a full understanding of alternative physical mechanisms for decadal and centennial climate change is required both in the pre- and postindustrial epochs before the circumstantial evidence for solar forcing can be dismissed with impunity.

A significant limitation in reducing uncertainties in the climate response to the sun's changing radiation is the lack of reliable observational knowledge of the amplitude of solar irradiance changes other than during one recent 11-yr cycle. Not well recognized, in particular, are limitations of the sunspot number record as a surrogate for irradiance variability. If longer-term irradiance variations are indeed occurring, they are not tracked by the sunspot number, which lacks a long-term trend, reflecting the failure of sunspots to account for solar variability mechanisms beyond those associated with activity complexes on the disk (e.g., the variations in the background facular emission from the network that is a postulated source of irradiance variability beyond the range exhibited by the contemporary sun, White et al. 1992). Since different spectral regions impact different aspect of the climate system, also necessary for proper specification of climate forcing by changing solar radiation is knowledge of the spectral dependence of the radiation, which remains thus far observationally undefined at wavelengths longer than 400 nm.

Definitive answers about long-term solar irradiance variability require continuous, uninterrupted solar monitoring by space-based instruments that are cross-calibrated to maintain adequate long-term precision over many decades. Seventeen years of solar monitoring is too short for anything but speculation about the reality and magnitude of long-term irradiance variability. Unless (until) the reality of longer-term solar irradiance variations is established it will be difficult to evaluate whether the correlations among solar and climate parameters are coincident or causal, or whether simulations of climate change using irradiance reconstruction like those postulated in Fig. 13 are relevant. Proposed reductions in environmental monitoring and the lack of access to space threaten to jeopardize the present solar monitoring database by a data gap (which would preclude cross calibration of existing and future data) or termination of the record; present plans are not yet sufficiently secure to ensure a reliable record of solar irradiance for the foreseeable future. Lacking the requisite long-term solar database, uncertainty about solar influences on climate change may well persist indefinitely. Although inferences have been made about long-term solar variability from comparisons with sunlike stars and cosmogenic isotope records, such circumstantial evidence is incapable of ever providing the certainty needed for policy making regarding the sun's influence (or lack of) on global climate change (see, e.g., Foukal 1994 for a discussion of ambiguities in the interpretation of sunlike stars).

Assuming the validity of long-term solar irradiance variations deduced from monitoring of solar and stellar variability, seen in Fig. 13 to track the cosmogenic isotope changes, the reconstruction suggests that solar radiation changes may have been the predominant climate forcing during the seventeenth and eighteenth centuries. But according to a simple linear parameterization of surface temperature anomalies and solar irradiance based on this preindustrial relationship, less than one-third of the earth's surface warming since 1970 is attributable to changing solar radiation. Presumably this reflects the increasing dominance in the past century of anthropogenic climate forcing relative to natural solar-induced variations. Cosmogenic isotope records suggest that contemporary solar activity levels are now approaching historically high levels, last seen in the thirteenth century medieval solar activity maximum (see Figs. 11 and 15). Activity levels of the present-day sun are as high as one-third of the brightest sunlike stars. This evidence from both cosmogenic isotopes and sun-

like stars points to the likelihood of future solar activity falling to lower levels, rather than increasing. Extrapolation of periodicities present in cosmogenic isotope data infer that this decrease may commence around 2030 (Jirikowic and Damon 1994), after which time the detectability of greenhouse climate forcing should further improve relative to natural solar induced variability.

Even in the event that solar radiation changes are eventually well specified, additional work is needed to understand the impact of this radiation on the climate system in such a way that decadal and centennial variations are fully understood regionally and globally in different epochs. This will likely require time-dependent simulations over past centuries, in the present, and into the future, with GCMs appropriately coupled to middle-atmosphere models, utilizing realistic spectrally dependent variations with properly parameterized wavelength-dependent impact on the climate system. Importantly, analysis of paleoclimate data from over the globe must be integrated into the assessment of the results of the simulations. Such studies are only just beginning. Sun–climate studies in the future require cross-disciplinary endeavors such as promoted and conceived by PACLIM and ARRCC.

Acknowledgments. Data used in this paper were kindly provided by Doug Hoyt, Dick Willson, Ray Bradley, Juerg Beer, Minze Stuiver, and Melissa Free. Bill Marquette supplied the BBSO Ca images. The NSO produces the 1083-nm EW data. Dust veil index and CO_2 data were obtained from the CDIAC, Oak Ridge, and *UARS* UV irradiance data from the GSFC DAAC. Matthew O'Donnell of the British Meteorological Office provided the IPCC temperature data. J. Lean appreciates ongoing discussion about solar variability with Peter Foukal, Dick White, Gary Rottman, and Andy Skumanich, and thanks Tim Baumgartner for the opportunity to participate in the 1995 PACLIM. Recent discussions with Warren White and Dan Cayan about sea surface temperatures are happily acknowledged. The Strategic Environmental Research and Development Program (SERDP) and NOAA provided partial funding support.

REFERENCES

Allen, M. R., and L. A. Smith, 1994: Investigating the origins and significance of low-frequency modes of climate variability. *Geophys. Res. Lett.,* **21,** 883–886.

Anderson, R. Y., 1992: Possible connection between surface winds, solar activity and the earth's magnetic field. *Nature,* **358,** 51–53.

Ardanuy, P. E., H. L. Kyle, and D. Hoyt, 1992: Global relationships among the earth's radiation budget, cloudiness, volcanic aerosols, and surface temperature. *J. Climate,* **5,** 1120–1139.

Auclair, A. N. D., 1992: Forest wildfire, atmospheric CO_2 and solar irradiance periodicity. *Eos, Trans. Amer. Geophys. Union,* Suppl., p. 70.

Balachandran, N. K., and D. Rind, 1995: Modeling the effects of UV variability and the QBO on the troposphere–stratosphere system. Part I: The middle atmosphere. *J. Climate,* **8,** 2058–2079.

Baldwin, M. P., and T. J. Dunkerton, 1989: Observations and statistical simulations of a proposed solar cycle/QBO/weather relationships. *Geophys. Res. Lett.,* **16,** 863–866.

Baliunas, S., and R. Jastrow, 1990: Evidence for long-term brigthness changes of solar-type stars. *Nature,* **348,** 520–523.

Barnett, T. P., 1989: A solar–ocean relation: Fact or fiction? *Geophys. Res. Lett.,* **16,** 803–806.

Beer, J., U. Siegenthaler, G. Bonani, R. C. Finkel, H. Oeschger, M. Suter, and W. Wolfli, 1988: Information on past solar activity and geomagnetism from ^{10}Be in the Camp Century ice core. *Nature,* **331,** 675–679.

——, and Coauthors, 1994: Solar variability traced by cosmogenic isotopes. *The Sun as a Variable Star,* J. M. Pap, C. Fröhlich, H. S. Hudson, and S. K. Solanki, Eds., Cambridge University Press, 291–300.

Bradley, R. S., Ed., 1991: *Global Changes of the Past.* UCAR/Office for Interdisciplinary Earth Studies, Global Change Institute, Boulder, CO, 514 pp.

——, and P. D. Jones, 1993: ''Little Ice Age'' summer temperature variations: Their nature and relevence to recent global warming trends. *The Holocene,* **3**, 367–376.

Briffa, K. R., T. S. Bartholin, D. Eckstein, P. D. Jones, W. Karlen, F. H. Schweingruber, and P. Zetterberg, 1990: A 1,400-year tree-ring record of summer temperatures in Fennoscandia. *Nature,* **346,** 434–439.

Burroughs, W. J., 1992: *Weather Cycles Real or Imaginary.* Cambridge University Press, 207 pp.

Chandra, S., and R. D. McPeters, 1994: The solar cycle variation of ozone in the stratosphere inferred from Nimbus 7 and NOAA 11 satellites. *J. Geophys. Res.,* **99,** 20 665–20 671.

——, J. L. Lean, O. R. White, D. K. Prinz, G. R. Rottman, and G. E. Brueckner, 1995: Solar UV irradiance variability during the declining phase of solar cycle 22. *Geophys. Res. Lett.,* **22,** 2481–2484.

Cohen, T. J., and E. I. Sweester, 1975: The ''spectra'' of the solar cycle and of data for Atlantic tropical cyclones. *Nature,* **256,** 295–296.

Crowley, T. J., and K.-Y. Kim, 1993: Towards development of a strategy for determining the origin of decadal-centennial climate variability. *Quat. Sci. Rev.,* **12,** 375–385.

——, and ——, 1995: Comparison of proxy records of climate change and solar forcing. *Geophys. Res. Lett.,* **22,** 933–936.

——, T. A. Criste, and N. R. Smith, 1993: Reassessment of Crête (Greenland) Ice core acidity/volcanism link to climate change. *Geophys. Res. Lett.,* **20,** 209–212.

Currie, R. G., and O'Brien, 1988: Periodic 18.6 year and cycle 10- to 11-year signals in northeast United States precipitation data. *Int. J. Climatol.,* **8,** 255–281.

Damon, P. E., and J. L. Jirikowic, 1994: Solar forcing of global climate change. *The Sun as a Variable Star,* J. M. Pap, C. Fröhlich, H. S. Hudson, and S. K. Solanki, Eds., Cambridge University Press, 301–314.

Dansgaard, W., S. J. Johnson, H. B. Clausen, D. Dahl-Jensen, N. Gundestrup, C. H. Hammer, and H. Oeschger, 1984: North Atlantic oscillations revealed by deep Greenland ice cores. *Climate Processes and Climate Sensitivity, Geophys. Monogr.,* No. 29, Amer. Geophys. Union, 288–298.

de Gruijl, F. R., 1995: Impacts of a projected depletion of the ozone layer. *Consequences,* **1,** 13–21.

de Vries, H., 1958: Variations in concentrations of radiocarbon with time and location on Earth. *Proc. Koninkl Nederlandse Adak. Wet. Ser B.,* **61,** 94–102.

Denton, G. H., and W. Karlen, 1973: Holocene climatic varations—their pattern and possible causes. *Quat. Res.,* **3,** 155–205.

Dunbar, R. B., G. M. Wellington, M. W. Colgan, and P. W. Glynn, 1994: Eastern Pacific sea surface temperature since 1600 A.D.: The δ ^{18}O record of climate variability in Galápagos coral. *Paleoceanography,* **9,** 291–315.

Eddy, J. A., 1976: The Maunder Minimum. *Science,* **192,** 1189–1202.
——, 1977: The case of the missing sunspots. *Sci. Amer.,* **236,** 80–89.
Fiala, A. D., D. W. Dunham, and S. Sofia, 1994: Variation of the solar diameter from solar eclipse observations, 1715–1991. *Solar Phys.,* **152,** 97–104.
Fligge, M., and S. K. Solanki, 1997: Inter-cycle variations of solar irradiance: Sunspot areas as a pointer. *Solar Phys.,* **173**, 427–439.
Foukal, P., 1981: Sunspots and changes in the global output of the Sun. *The Physics of Sunspots,* L. E. Cram and J. H. Thomas, Eds., Sacramento Peak Observatory, 391 pp.
——, 1990: *Solar Astrophysics.* John Wiley and Sons, 475 pp.
——, 1994: Stellar luminosity variations and global warming. *Science,* **264,** 238–239.
——, and J. Lean, 1988: Magnetic modulation of solar luminosity by photospheric activity. *Astrophys. J.,* **328,** 347–357.
——, and ——, 1990: An empirical model of total solar irradiance variation between 1874 and 1988. *Science,* **247,** 556–558.
Friis-Christensen, E., and K. Lassen, 1991: Length of the solar cycle: An indicator of solar activity closely associated with climate. *Science,* **254,** 698–700.
Fröhlich, C., P. V. Foukal, J. R. Hickey, H. S. Hudson, and R. C. Willson, 1991: Solar irradiance variability from modern measurements. *The Sun in Time,* C. P. Sonett, M. S. Giampapa, and M. S. Matthews, Eds., The University of Arizona Press, 11–29.
——, and Coauthors, 1997: In-flight performance of the VIRGO solar irradiance instrument on SOHO. *Solar Phys.,* **175**, 267–286.
George C. Marshall Institute, 1989: *Scientific Perspectives on the Greenhouse Problem.* George C. Marshall Institute, 37 pp.
Gilliland, R. L., 1981: Solar radius variations over the past 265 years. *Astrophys. J.,* **248,** 1144–1155.
Grootes, P. M., and M. Stuiver, 1997: Oxygen 18/16 variability in Greenland snow and ice with 10^{-3} to 10^{-5}-year time resolution. *J. Geophys. Res.,* **102**, 26 455–26 470.
Haigh, J. D., 1994: The role of stratospheric ozone in modulating the solar radiative forcing of climate. *Nature,* **370,** 544–546.
——, 1996: The impact of solar variability on climate. *Science,* **272,** 961–984.
Halfman, J. D., and T. C. Johnson, 1988: High-resolution record of cyclic climatic change during the past 4 ka from Lake Turkana, Kenya. *Geology,* **16,** 496–500.
Hameed, S., 1984: Fourier analyis of Nile flood levels. *Geophys. Res. Lett.,* **1,** 843–845.
——, W. M. Yeh, M. T. Li, R. D. Cess, and W. C. Wang, 1983: An analysis of periodicities in the 1470 to 1974 Beijing precipitation record. *Geophys. Res. Lett.,* **10,** 436–439.
Hannah, L., D. Lohse, C. Hutchinson, J. L. Carr, and A. Lankerani, 1994: A preliminary inventory of human disturbances of world ecosystems. *Ambio,* **XXIII,** 246–250.
Hansen, J. E., and A. A. Lacis, 1990: Sun and dust versus greenhouse gases. *Nature,* **346,** 713–719.
——, G. Russell, D. Rind, P. Stone, A. Lacis, S. Lebedoff, R. Ruedy, and L. Travis, 1983: Efficient three-dimensional global models for climate studies: Models I and II. *Mon. Wea. Rev.,* **111,** 609–662.
——, A. Lacis, D. Rind, G. Russell, P. Stone, I. Fung, R. Reudy, and J. Lerner, 1984: Climate sensitivity: Analysis of feedback mechanisms. *Climate Processes and Climate Sensitivity, Geophys. Monogr.,* No. 29, Amer. Geophys. Union, 130–163.
——, G. Russell, A. Lacis, I. Fung, D. Rind, and P. Stone, 1985: Climate response times: Dependence on climate sensitivity and ocean mixing mechanisms. *Science,* **229,** 857–859.
——, A. Lacis, R. Ruedy, M. Sato, and H. Wilson, 1993: How sensitive is the world's climate? *Natl. Geogr. Res. Explor.,* **9,** 143–158.
Hartmann, D. L., 1994: *Global Physical Climatology.* International Geophysics Series, Vol. 56, Academic Press.
Hood, L. L., 1997: The solar cycle variation of total ozone: Dynamical forcing in the lower stratosphere. *J. Geophys. Res.,* **102,** 1355–1370.
——, and J. P. McCormack, 1992: Components of interannual ozone change based on Nimbus 7 TOMS data. *Geophys. Res. Lett.,* **19,** 2309–2312.
——, J. Jirikowic, and J. P. McCormack, 1993: Quasi-decadal variability of the stratosphere: Influence of long term solar ultraviolet variations. *J. Atmos. Sci.,* **50,** 3941–3958.
Houghton, J. T., B. A. Callander, and S. K. Varney, Eds., 1992: *Climate Change 1992.* The Supplementary Report to the IPCC Scientific Assessment, Cambridge University Press, 200 pp.
——, L. G. Meira Filhon, J. Bruce, H. Lee, B. A. Callander, E. Haites, N. Harris, and K. Maskell, Eds., 1995: *Climate Change 1994.* Radiative Forcing of Climate Change and An Evaluation of the IPCC IS92 Emission Scenarios, Cambridge University Press, 339 pp.
Hoyt, D. V., and K. H. Schatten, 1993: A discussion of plausible solar irradiance variations, 1700–1992. *J. Geophys. Res.,* **98,** 18 895–18 906.
——, and ——, 1997: *The Role of the Sun in Climate Change.* Oxford University Press, 279 pp.
——, H. L. Kyle, J. R. Hickey, and R. H. Maschhoff, 1992: The Nimbus 7 solar total irradiance: A new algorithm for its derivation. *J. Geophys. Res.,* **97,** 51–63.
——, K. H. Schatten, and E. Nesmes-Ribes, 1994: The one hundredth year of Rudolf Wolf's death: Do we have the correct reconstruction of solar activity? *Geophys. Res. Lett.,* **21,** 2067–2070.
Hudson, H. S., 1988: Observed variability of the solar luminosity. *Annu. Rev. Astron. Astrophys.,* **26,** 473–507.
——, S. Silva, M. Woodard, and R. C. Willson, 1982: The effects of sunspots on solar irradiance. *Solar Phys.,* **76,** 211–219.
Hughes, M. K., and H. F. Diaz, 1994: The Medieval warm period. *Climate Change,* **26,** 2–3.
James, I. N., and P. M. James, 1989: Ultra-low-frequency variability in a simple atmospheric circulation model. *Nature,* **342,** 53–55.
Jirikowic, J. L., and P. E. Damon, 1994: The Medieval solar activity maximum. *Climate Change,* **26,** 309–316.
Joselyn, J., 1995: Geomagnetic activity forecasting: The state of the art. *Rev. Geophys.,* **33,** 383–401.
Karl, T. R., and W. E. Riebsame, 1984: The identification of 10- to 20-year temperature and precipitation fluctutations in the contiguous United States. *J. Climate Appl. Meteor.,* **23,** 950–966.
Keeling, C. D., and T. P. Whorf, 1994: Atmospheric CO_2 records from sites in the SIO air sampling network. *Trends '93: A Compendium of Data on Global Change,* T. A. Boden, D. P. Kaiser, R. J. Sepanski, and F. W. Stoss, Eds., Oak Ridge National Laboratory, 16–26.
Kelly, P. M., 1977: Solar influences on North Atlantic mean sea level pressure. *Nature,* **269,** 320–322.
——, and T. M. L. Wigley, 1992: Solar cycle length, greenhouse forcing and global climate. *Nature,* **360,** 328–330.
Kuhn, J. R., and K. G. Libbrecht, 1991: Nonfacular solar luminosity variations. *Astrophys. J.,* **381,** L35–L37.
Kuo, C., C. Lindberg, and D. J. Thomson, 1990: Coherence established between atmospheric carbon dioxide and global temperature. *Nature,* **343,** 709–714.
Labitzke, K., and H. van Loon, 1990: Associations between the 11-year solar cycle, the quasi-biennial oscillation and the atmosphere: A summary of recent work. *Philos. Trans. Roy. Soc. London,* **330A,** 577–589.
——, and ——, 1993a: Some recent studies of probable connections between solar and atmospheric variability. *Ann. Geophys.,* **11,** 1084–1094.
——, and ——, 1993b: Aspects of a decadal sun–atmosphere connection. *The Solar Engine and its Influence on Terrestrial Atmosphere and Climate,* E. Nesme-Ribes, Ed., ASI Series I: Global Environemental Change, Vol. 25, NATO, 381–393.
Lacis, A. A., D. J. Wuebbles, and J. A. Logan, 1990: Radiative forcing of climate by changes in the vertical distribution of ozone. *J. Geophys. Res.,* **95,** 9971–9981.

Lamb, H. H., 1977: Supplementary volcanic dust veil assessments. *Climate Monitor,* **6,** 57–67.
Lau, K.-M., and H. Weng, 1995: Climate signal detection using wavelet transform: How to make a time series sing. *Bull. Amer. Meteor. Soc.,* **76,** 2391–2402.
Lean, J., 1989: Contribution of ultraviolet irradiance variations to changes in the sun's total irradiance. *Science,* **244,** 197–200.
——, 1991: Variations in the sun's radiative output. *Rev. Geophys.,* **29,** 505–535.
——, 1997: The sun's radiation and its relevance for earth. *Annu. Rev. Astron. Astrophys,* **35,** 33–67.
——, A. Skumanich, and O. White, 1992: Estimating the sun's radiative output during the Maunder Minimum. *Geophys. Res. Lett.,* **19,** 1591–1594.
——, O. R. White, and A. Skumanich, 1995a: On the solar ultraviolet spectral irradiance during the Maunder Minimum. *Global Biogeochem. Cycles,* **9,** 171–182.
——, J. Beer, and R. Bradley, 1995b: Reconstruction of solar irradiance since 1610: Implications for climate change. *Geophys. Res. Lett.,* **22,** 3195–3198.
——, G. J. Rottman, H. L. Kyle, T. N. Woods, J. R. Hickey, and L. C. Puga, 1997: Detection and parameterization of variations in solar mid and near ultraviolet radiation (200 to 400 nm). *J. Geophys. Res.,* **102,** 29 939–29 956.
——, J. Cook, W. Marquette, and A. Johannesson, 1998: Magnetic modulation of the solar irradiance cycle. *Astrophys. J.,* **492,** 390–401.
Lee, R. B., III, M. A. Gibson, R. S. Wilson, and S. Thomas, 1995: Long-term total solar irradiance variability during sunspot cycle 22. *J. Geophys. Res.,* **100,** 1667–1675.
Livingston, W. C., L. Wallace, and O. R. White, 1988: Spectrum line intensity as a surrogate for solar irradiance variations. *Science,* **240,** 1765–1767.
Lockwood, G. W., B. A. Skiff, S. L. Baliunas, and R. R. Radick, 1992: Long term solar brightness changes estimated from a survey of Sun-like stars. *Nature,* **360,** 653–655.
London, J., G. J. Rottman, T. N. Woods, and F. Wu, 1993: Time variations of solar UV irradiance as measured by the SOLSTICE (UARS) instrument. *Geophys. Res. Lett.,* **20,** 1315–1318.
Luther, M. R., R. B. Lee III, B. R. Barkstron, J. E. Cooper, R. D. Cess, and C. H. Duncan, 1986: Solar calibration results from two earth radiation budget nonscanner instruments. *Appl. Opt.,* **25,** 540–545.
Mann, M. E., and J. Park, 1994: Global-scale modes of surface temperature variability on interannual to century timescales. *J. Geophys. Res.,* **99,** 25 819–25 833.
Mason, B. J., 1976: Towards the understanding and prediction of climatic variations. *Quart. J. Roy. Meteor. Soc.,* **102,** 478–498.
McHargue, L. R., and P. E. Damon, 1991: The global beryllium 10 cycle. *Rev. Geophys.,* **29,** 141–158.
Mehta, V. M., and T. Delworth, 1995: Decadal variability of the tropical Atlantic ocean surface temperature in shipboard measurements and in a global ocean–atmosphere model. *J. Climate,* **8,** 172–190.
Mitchell, J. M., Jr., 1976: An overview of climatic variability and its causal mechanisms. *Quat. Res.,* **6,** 481–493.
——, C. W. Stockton, and D. M. Meko, 1979: Evidence of a 22-year rhythm of drought in the western United States related to the Hale solar cycle since the 17th century. *Solar Terrestrial Influences on Weather and Climate,* B. M. McCormac and T. A. Seliga, Eds., D. Reidel, 124–144.
NRC, 1994: *Solar Influences on Global Change.* National Academy Press, 163 pp.
Nesme-Ribes, E., E. N. Ferreira, R. Sadourny, H. Le Truet, and Z. X. Li, 1993: Solar dynamics and its impact on solar irradiance and the terrestrial climate. *J. Geophys. Res.,* **98,** 18 923–18 935.
Newell, N. E., R. E. Newell, J. Hsuing, and W. Zhongxiang, 1989: Global marine temperature variation and the solar magnetic cycle. *Geophys. Res. Lett.,* **16,** 311–314.
North, G. R., and K.-Y. Kim, 1995: Detection of forced climate signals. Part II: Simulation results. *J. Climate,* **8,** 409–417.
Parker, D. E., P. D. Jones, C. K. Folland, and A. Bevan, 1994: Interdecadal changes of surface temperature since the late nineteenth century. *J. Geophys. Res.,* **99,** 14 373–14 399.
Penner, J. E., and Coauthors, 1994: Quantifying and minimizing uncertainty of climate forcing by anthropogenic aerosols. *Bull. Amer. Meteor. Soc.,* **75,** 375–400.
——, T. M. L. Wigley, P. Jaumann, B. D. Santer, and K. E. Taylor, 1995: Anthropogenic aerosols and climate change: A method for calibrating forcing. *Assessing Climate Change—The Story of the Model Evaluation Consortium for Climate Assessment,* Lawrence Livermore National Laboratory, Publ. UCRL-JC-124338.
Perry, C. A., 1994: Solar-irradiance variations and regional precipitation fluctuations in the western USA. *Int. J. Climatol.,* **14,** 969–983.
Pestiaux, P., J. C. Duplessy, and A. Berger, 1987: Paleoclimatic variability at frequencies ranging from 10^{-4} cycle per year to 10^{-3} cycle per year—Evidence for nonlinear behavior of the climate system. *Climate Processes and Climate Sensitivity,* M. R. Rampino, J. E. Sanders, W. S. Newman, and L. K. Konigsson, Eds., Van Nostrand Reinhold, 285–299.
Peterson, L. C., J. T. Overpeck, N. Kipp, and J. Imbrie, 1991: A high resolution late-quaternary upwelling record from the anoxic Cariaco Basin, Venezuela. *Paleoceanography,* **6,** 99–119.
Phillips, P., and I. M. Held, 1994: The response to orbital perturbations in an atmospheric model coupled to a slab ocean. *J. Climate,* **7,** 767–782.
Pittock, A. B., 1979: Solar cycles and the weather: Successful experiments in autosuggestion? *Solar-Terrestrial Influences on Weather and Climate,* B. M. McCormac and T. A. Selida, Eds., D. Reidel, 181–191.
Pollack, J. B., W. J. Borucki, and O. B. Toon, 1979: Are solar spectral variations a drive for climatic change? *Nature,* **282,** 600–603.
Reid, G., 1991: Solar total irradiance variations and the global sea surface temperature record. *J. Geophys. Res.,* **96,** 2835–2844.
Reinsel, G. C., W.-K. Tam, and L. H. Ying, 1994: Comparison of trend analyses for Umkehr data using new and previous inversion algorithms. *Geophys. Res. Lett.,* **21,** 1007–1010.
Rind, D., and J. Overpeck, 1993: Hypothesized causes of decade-to-century climate variability: Climate model results. *Quat. Sci. Rev.,* **12,** 357–374.
——, and N. K. Balachandran, 1995: Modeling the effects of UV variability and the QBO on the troposphere–stratosphere system. Part II: The troposphere. *J. Climate,* **8,** 2080–2095.
——, D. Peteet, and G. Kukla, 1989: Can Milankovitch orbital variations initiate the growth of ice sheets in a general circulation model? *J. Geophys. Res.,* **94,** 12 851–12 871.
Robock, A., 1979: The ''Little Ice Age'': Northern hemisphere average observations and model calculations. *Nature,* **206,** 1402–1404.
——, and M. P. Free, 1995: Ice cores as an index of global volcanism from 1850 to the present. *J. Geophys. Res.,* **100,** 11 549–11 567.
Rottman, G. J., 1988: Observations of solar UV and EUV variability. *Adv. Space Res.,* **8,** (7)53–(7)66.
Salby, M. L., and D. J. Shea, 1991: Correlations between solar activity and the atmosphere: An unphysical explanation. *J. Geophys. Res.,* **96,** 22 579–22 595.
Sato, M., J. E. Hansen, M. P. McCormick, and J. B. Pollack, 1993: Stratospheric aerosol optical depths, 1850–1990. *J. Geophys. Res.,* **98,** 22 987–22 994.
Schatten, K. H., and J. A. Orosz, 1990: Solar constant secular changes. *Solar Phys.,* **125,** 179–184.
Schlesinger, M. E., and N. Ramarnkutty, 1992: Implications for global warming of intercycle solar irradiance variations. *Nature,* **360,** 330–333.
Schwarzkopf, M. D., and V. Ramaswamy, 1993: Radiative forcing due to ozone in the 1980's: Dependence on altitude of ozone change. *Geophys. Res. Lett.,* **20,** 205–208.
Seleshi, Y., G. R. Demarée, and J. W. Delleur, 1994: Sunspot numbers

as a possible indicator of annual rainfall at Addis Ababa, Ethiopia. *Int. J. Climatol.,* **14,** 911–923.

Sofia, S., and P. Fox, 1994: Solar variability and climate. *Climate Change,* **30,** 1–9.

Solanki, S. K., and Y. C. Unruh, 1998: A model of the wavelength dependence of solar irradiance variations. *Astron. Astrophys.,* **329,** 747–754.

Stevens, M. J., and G. R. North, 1996: Detection of the climate response to the solar cycle. *J. Atmos. Sci.,* **53,** 2594–2608.

Stuiver, M., and T. F. Braziunas, 1993: Sun, ocean, climate and atmosphere $^{14}CO_2$: An evaluation of causal and spectral relationships. *The Holocene,* **3,** 289–305.

——, and P. J. Reimer, 1993: Extended ^{14}C data base and revised CALIB 3.0 ^{14}C age calibration program. *Radiocarbon,* **35,** 215–230.

Thompson, L. G., E. Mosley-Thompson, M. E. Davis, T. Yao, P. N. Lin, and J. Dai, 1993: New evidence for recent warming from high resolution Chinese and Peruvian ice cores. *Eos, Trans. Amer. Geophys. Union,* Suppl., p. 90.

Tinsley, B. A., 1988: The solar cycle and the QBO influences on the latitude of storm tracks in the North Atlantic. *Geophys. Res. Lett.,* **15,** 409–412.

Visser, H., and J. Molenaar, 1995: Trend estimation and regression analysis in climatological time series: An application of structural time series models and the Kalman filter. *J. Climate,* **8,** 969–979.

White, O. R., G. J. Rottman, and W. C. Livingston, 1990: Estimation of the solar Lyman alpha flux from ground based measurements of the Ca II K line. *Geophys. Res. Lett.,* **17,** 575–578.

——, A. Skumanich, J. Lean, W. C. Livingston, and S. Keil, 1992: The sun in a non-cycling state. *Public. Astron. Soc. Pacif.,* **104,** 1139–1143.

White, W. B., J. Lean, D. R. Cayan, and M. D. Dettinger, 1997: Response of global upper ocean temperature to changing solar irradiance. *J. Geophys. Res.,* **102,** 3255–3266.

Wigley, T. M. L., and P. M. Kelly, 1990: Holocene climatic change, ^{14}C wiggles and variations in solar irradiance. *Philos. Trans. Roy. Soc. London,* **330A,** 547–560.

——, and S. C. B. Raper, 1990: Climatic change due to solar irradiance changes. *Geophys. Res. Lett.,* **17,** 2169–2172.

Wilson, O. C., 1978: Chromospheric variations in main sequence stars. *Astrophys. J.,* **226,** 379–396.

Willson, R. C., and H. S. Hudson, 1991: A solar cycle of measured and modeled total irradiance. *Nature,* **351,** 42–44.

Woods, T. N., and Coauthors, 1996: Validation of the UARS solar ultraviolet irradiances: Comparison with the ATLAS-1, -2 measurements. *J. Geophys. Res.,* **101,** 9541–9569.

Wuebbles, D., J. Douglas, E. Kinnison, K. E. Grant, and J. Lean, 1991: The effect of solar flux variations and trace gas emissions on recent trends in stratospheric ozone and temperature. *J. Geomagn. Geoelectr.,* **43** (Suppl.), 709–718.

Zhang, Q., W. H. Soon, S. L. Baliunas, G. W. Lockwood, B. A. Skiff, and R. R. Radick, 1994: A method of determining possible brightness variations of the sun in past centuries from observations of solar-type stars. *Astrophys. J.,* **427,** L111–L114.